PAPER

Design, synthesis and binding properties of a fluorescent $\alpha_9\beta_1/\alpha_4\beta_1$ integrin antagonist and its application as an *in vivo* probe for bone marrow haemopoietic stem cells†

Benjamin Cao,[a] Oliver E. Hutt,[a] Zhen Zhang,[a] Songhui Li,[a] Shen Y. Heazlewood,[a] Brenda Williams,[a] Jessica A. Smith,[a] David N. Haylock,[a,b] G. Paul Savage*[a] and Susan K. Nilsson[a,b]

The $\alpha_9\beta_1$ and $\alpha_4\beta_1$ integrin subtypes are expressed on bone marrow haemopoietic stem cells and have important roles in stem cell regulation and trafficking. Although the roles of $\alpha_4\beta_1$ integrin have been thoroughly investigated with respect to HSC function, the role of $\alpha_9\beta_1$ integrin remains poorly characterised. Small molecule fluorescent probes are useful tools for monitoring biological processes *in vivo*, to determine cell-associated protein localisation and activation, and to elucidate the mechanism of small molecule mediated protein interactions. Herein, we report the design, synthesis and integrin-dependent cell binding properties of a new fluorescent $\alpha_9\beta_1$ integrin antagonist (R-BC154), which was based on a series of *N*-phenylsulfonyl proline dipeptides and assembled using the Cu(ı)-catalyzed azide alkyne cyclo-addition (CuAAC) reaction. Using transfected human glioblastoma LN18 cells, we show that R-BC154 exhibits high nanomolar binding affinities to $\alpha_9\beta_1$ integrin with potent cross-reactivity against $\alpha_4\beta_1$ integrin under physiological mimicking conditions. On-rate and off-rate measurements revealed distinct differences in the binding kinetics between $\alpha_9\beta_1$ and $\alpha_4\beta_1$ integrins, which showed faster binding to $\alpha_4\beta_1$ integrin relative to $\alpha_9\beta_1$, but more prolonged binding to the latter. Finally, we show that R-BC154 was capable of binding rare populations of bone marrow haemopoietic stem and progenitor cells when administered to mice. Thus, R-BC154 represents a useful multi-purpose fluorescent integrin probe that can be used for (1) screening small molecule inhibitors of $\alpha_9\beta_1$ and $\alpha_4\beta_1$ integrins; (2) investigating the biochemical properties of $\alpha_9\beta_1$ and $\alpha_4\beta_1$ integrin binding and (3) investigating integrin expression and activation on defined cell phenotypes *in vivo*.

[a]*CSIRO Materials Science and Engineering, Bag 10, Clayton Sth MDC, VIC 3169, Australia. E-mail: Paul.Savage@csiro.au; Fax: +61 3 9543 2376; Tel: +61 3 9545 2523*
[b]*Australian Regenerative Medicine Institute, Monash University, Wellington Rd, Clayton, VIC 3800, Australia*

†Electronic supplementary information (ESI) available: Supplementary figures S1–3 and copies of ^{1}H, ^{13}C, COSY and HSQC NMR spectra. See DOI: 10.1039/c3ob42332h

Introduction

Integrins are non-covalently linked $\alpha\beta$ heterodimeric transmembrane proteins that function primarily as mediators of cell adhesion and cell signalling processes.[1] Owing to their roles in tumour development, metastasis and haemostasis, integrins have been inextricably linked to several pathological conditions including cancer, infection, thrombosis and autoimmune disease and are acknowledged therapeutic targets for small molecule intervention.[2,3]

In mammals, 18 α-chains and 8 β-chains have been identified, with 24 different and unique $\alpha\beta$ combinations described to date.[4] The $\alpha_4\beta_1$ integrin (very late antigen-4; VLA-4) is expressed primarily on leukocytes and are known to be receptors for vascular cell adhesion molecule-1 (VCAM-1), fibronectin and osteopontin (Opn).[5,6] The $\alpha_4\beta_1$ integrin is a key regulator of leukocyte recruitment, migration and activation and has important roles in inflammation and autoimmune disease.[7] Accordingly, significant effort has been focused on the development of small molecule inhibitors of $\alpha_4\beta_1$ integrin function for the treatment of asthma, multiple sclerosis and Crohn's disease, with several candidates progressing to phase I and II clinical trials.[8] The related β_1 integrin, $\alpha_9\beta_1$, shares many of the structural and functional properties as $\alpha_4\beta_1$ and also binds to several of the same ligands including VCAM-1 and Opn.[9–12] Additionally, $\alpha_9\beta_1$ integrin are receptors for vascular endothelial growth factors (VEGF), nerve growth factor (NGF) and tenascin-C.[11,13,14] Unlike $\alpha_4\beta_1$, which has a restricted expression that is largely on leukocytes, the cellular

This journal is © The Royal Society of Chemistry 2014

Org. Biomol. Chem., 2014, **12**, 965–978 | 965

expression of $\alpha_9\beta_1$ is widespread and there is evidence to support its involvement in wound healing, angiogenesis and tumour development.[12,14–16]

Previously, both $\alpha_4\beta_1$ and $\alpha_9\beta_1$ integrins have been shown to be expressed by haemopoietic stem cells (HSC), which are the bone marrow stem cells responsible for the production of all blood cells throughout life.[17–19] In this context, the integrins $\alpha_4\beta_1$ and $\alpha_9\beta_1$ are primarily involved in the sequestration and recruitment of HSC to the bone marrow as well as the maintenance of HSC quiescence, a key characteristic for long-term repopulating stem cells.[18] HSC regulation by $\alpha_4\beta_1$ and $\alpha_9\beta_1$ integrins is mediated through interactions with VCAM-1 and Opn, which are expressed and/or secreted by bone-lining osteoblasts, endothelial cells and other cells of the bone marrow environment.[18] Recently, DiPersio and co-workers identified a selective small molecule $\alpha_4\beta_1$ integrin antagonist, BIO5192 (1), which is capable of mobilising bone marrow HSC and progenitor cells into the peripheral circulation in mice. (Fig. 1).[20] This study validated small molecule inhibitors of $\alpha_4\beta_1$ integrin as effective HSC mobilisation agents, which may have potential applications in peripheral blood stem cell transplants for the treatment of blood disorders and cancers. Despite the structural and functional similarities between $\alpha_4\beta_1$ and $\alpha_9\beta_1$, the role of $\alpha_9\beta_1$ integrin in this regard remains unexplored.

While $\alpha_4\beta_1$ integrin has been rigorously studied within the medicinal chemistry community, $\alpha_9\beta_1$ integrin has received considerably less attention as a target for small molecule intervention. Our ongoing interests in $\alpha_9\beta_1$ integrin in HSC biology led us to pursue the development of a fluorescent small

molecule $\alpha_9\beta_1$ integrin antagonist, which we could use for *in vitro* screening applications to identify novel integrin inhibitors as potential HSC mobilisation agents and for *in vivo* binding experiments to identify cell phenotypes that are targeted by this class of inhibitors. In the search for a suitable small-molecule that could be adapted for fluorescent labelling we identified the *N*-phenylsulfonyl proline peptidomimetic 2, which bears structural resemblance to BIO5192 (1) (Fig. 1).[12] In contrast to BIO5192 (1), which is a potent and selective $\alpha_4\beta_1$ antagonist, compound 2 is a sub-nanomolar inhibitor of $\alpha_9\beta_1$ but also shows potent cross reactivity against $\alpha_4\beta_1$ integrin.[12] In this seminal work, [35S]-labelled 2 was developed as a probe for investigating the functional differences between $\alpha_4\beta_1$ and $\alpha_9\beta_1$ integrins. While radiolabelling techniques are highly sensitive, issues associated with radioisotope labelling (costly, hazardous, difficult to handle and dispose, and isotope stability) make their applications restricted. Moreover, radiolabelled probes cannot be effectively used in a number of biological applications as they are not compatible with flow cytometry or standard microscopy techniques.

Herein we report the design, synthesis and binding properties of a fluorescent high-affinity small-molecule $\alpha_9\beta_1/\alpha_4\beta_1$ integrin probe that can be used for (1) *in vitro* inhibitor screening; (2) *in vitro* investigations of $\alpha_9\beta_1$ and $\alpha_4\beta_1$ integrin binding activity and (3) *in vivo* labelling experiments using multi-parameter flow cytometry. Interestingly, several potent $\alpha_2\beta_1$ integrin inhibitors such as 3, which also possess the *N*-phenylsulfonyl proline core scaffold have also been reported (Fig. 1).[21,22] Thus, any synthetic methodologies developed for fluorescent labelling of $\alpha_9\beta_1$ antagonists could also encompass $\alpha_4\beta_1$, $\alpha_4\beta_7$ and $\alpha_2\beta_1$ integrin antagonists.

Results and discussion

Design and synthesis of a fluorescent $\alpha_4\beta_1/\alpha_9\beta_1$ integrin probe

Our general strategy for the fluorescent labelling of compound 2 was based on established structure activity relationships (Fig. 2).[12,23] The pyrrolidine carbamate is important for ensuring high binding affinities to $\alpha_9\beta_1$ integrin and substitution of the tyrosine phenyl group is not well tolerated.[12] The acid functionality has been shown to be essential for activity.[24] While lipophilic substitution on the sulfonyl phenyl group is tolerated, the installation of a suitable linker at this position would
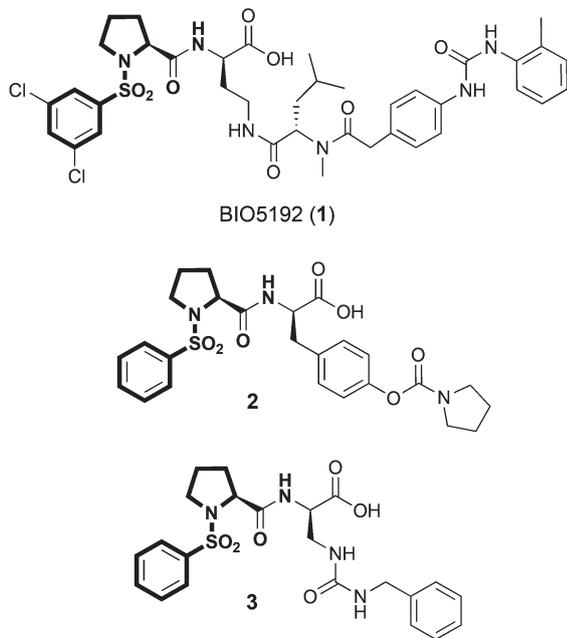

Fig. 1 Structures of $\alpha_4\beta_1$ selective integrin antagonist and HSC mobilisation agent 1 (BIO5192), $\alpha_9\beta_1/\alpha_4\beta_1$ integrin antagonist 2 and $\alpha_2\beta_1$ integrin antagonist 3. The common *N*-phenylsulfonyl proline core is highlighted in bold.
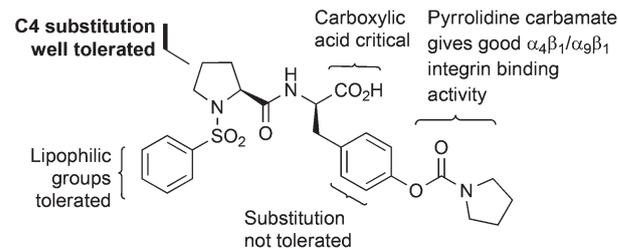

Fig. 2 Structure activity relationship for *N*-phenylsulfonyl proline-based $\alpha_9\beta_1$ integrin antagonists.

966 | *Org. Biomol. Chem.*, 2014, 12, 965–978

This journal is © The Royal Society of Chemistry 2014

not necessarily fulfil these requirements.[23] However, functionalisation with a wide range of substituents at the 4-position of the proline ring in the *trans*-configuration can be tolerated.[25,26] Thus, it was reasonable to suggest that incorporation of a suitable linker, such as a polyethylene glycol (PEG) linker at the C4-position of the proline residue would preserve the bioactive conformation of the dipeptide and provide distancing from the steric bulk of the fluorescent component. Therefore, our initial efforts focused on identifying an efficient strategy for installing a *trans*-configured bifunctional PEG linker at the C4-position of compound **2** for subsequent conjugation to a fluorescent tag.

We have previously reported on lactone **4** as a versatile synthon for accessing 4-*cis*-hydroxy proline based dipeptides through direct acylation with protected amino acids.[27] Subsequent activation of the 4-*cis*-hydroxy group followed by S_N2 displacement with nucleophiles would then provide the desired 4-*trans*-configured proline derivatives. Thus, we envisaged a variety of C4-functionalised derivatives of compound **2** could be acquired starting from lactone **4** and tyrosine derivative **7** (Scheme 1). Lactone **4** was readily prepared by treatment of *N*-phenylsulfonyl-*trans*-4-hydroxy-L-proline under Mitsunobu conditions employing DIAD and PPh$_3$.[27] The tyrosine derivative **7** was synthesised from protected **5** by treatment with pyrrolidine carbonyl chloride in the presence of K$_2$CO$_3$ to give intermediate **6**, followed by removal of the Cbz protecting group. Exposure of lactone **4** to tyrosine derivative **7** under biphasic conditions afforded the dipeptide **8** in 89% yield as a single diastereoisomer. This method takes advantage of the activated nature of the bicyclic lactone and allows clean conversion to the 4-*cis*-hydroxy proline dipeptides without resorting to dehydrative peptide coupling. Initial attempts in installing the PEG linker focused on the direct displacement of *cis*-configured triflate **9** with the amino PEG derivative **10**, which could be readily obtained from commercially accessible 4,7,10-trioxa-1,13-tridecanediamine.[28] S_N2 displacement of 4-*cis*-triflates with amines has been reported to give the corresponding *trans*-amino proline derivatives, which would be attractive in the current context given the low steric bulk of the resultant linkage.[26] Accordingly, the hydroxyl group of compound **8** was converted to the corresponding triflate **9** prior to treatment with the PEG derivative **10**, which gave the PEGylated product **11**, albeit in disappointing yields (27% over 2 steps) (Scheme 1).

Although no major side products were isolated during the formation of either the triflate **9**, or the PEG derivative **10**, a possible rationalisation for the poor yields of the N-alkylation reaction was intermediate formation of the trifluoromethanesulfonyl imidate. Therefore, the simplified *cis*-hydroxy compound **12**, which lacks a secondary amide was also investigated. Conversion of **12** to the corresponding triflate and then treatment with PEG amine **10** gave the *trans*-amino-proline derivative **13**, but again in a moderate 30% yield over two steps (Scheme 2a). This suggests concomitant formation of a trifluoromethanesulfonyl imidate intermediate is unlikely to be the principal cause for the low yields obtained for the
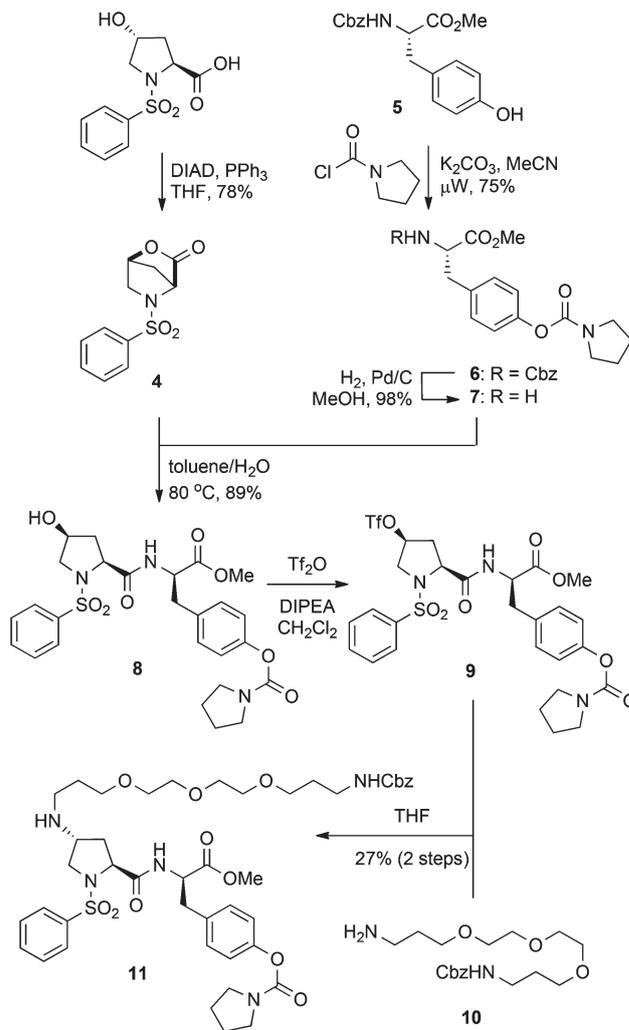
Scheme 1 Synthesis of PEGylated derivative **11** *via* triflate displacement approach.
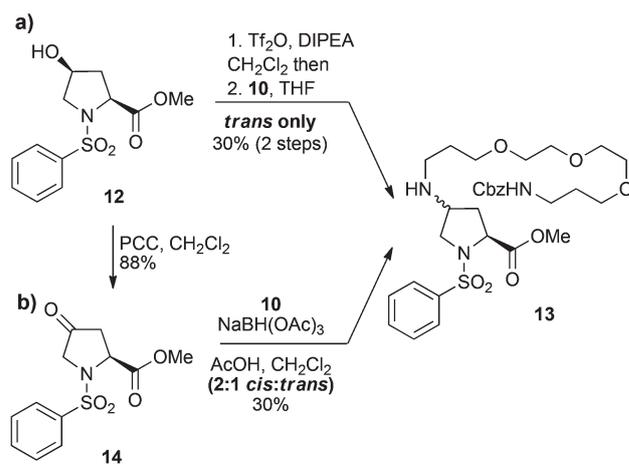
Scheme 2 Attempted *N*-alkylation of the C4 position of proline derivatives **12** and **14** with PEG amine **10** *via* (a) triflate displacement and (b) reductive amination, respectively.

PEGylation of dipeptide **9**. The poor reaction outcomes achieved from S_N2 displacement of triflate intermediates prompted us to pursue the derivative **13** *via* reductive amination of the ketone **14**. Thus, the ketone **14**, which was obtained from pyridinium chlorochromate (PCC) oxidation of alcohol **12**, was treated with $NaBH(OAc)_3$ and the PEG amine **10**, to give the desired **13** as the minor component of a 2:1 mixture of *cis*:*trans* isomers in a 30% yield (Scheme 2b). Thus, the poor yields observed for both direct displacement of *cis*-triflates and reductive amination using PEG amine substrates was attributed to a combination of low reaction efficiency and the recalcitrant nature of these compounds toward purification. Although we could repeatedly access the PEG-coupled compound **11**, the low yields made this sequence untenable and we sought more efficient strategies for incorporation of a PEG linker whilst preserving the bioactive nature of the dipeptide.

Reger and co-workers reported that introducing *N*-linked aromatic heterocycles (*e.g.* imidazoles, triazoles, tetrazoles and benzimidazoles) at the 4-position of the proline residue is well tolerated such that $\alpha_4\beta_1$ integrin binding activity was not detrimentally affected.[29] Based on this observation, we anticipated that attachment of a PEG linker *via* a triazole might also be tolerated for $\alpha_9\beta_1$ integrin binding. Consequently, this would allow installation of the PEG linker using the Cu(I)-catalyzed azide alkyne cycloaddition (CuAAC) reaction between an alkyne functionalised PEG derivative **15** and a *trans*-azido integrin antagonist **18** (Scheme 3).[30,31]

The alkyne functionalised PEG derivative **15** was obtained in one step from **10** by condensation with propionic acid under DCC coupling conditions (Scheme 3a). The synthesis of *trans*-azido functionalised dipeptide **18** was readily achieved from lactone **4** (Scheme 3b). Treatment of **4** with Na_2CO_3 in MeOH afforded the *cis*-hydroxy proline ester **12** in 80% yield. The *cis*-alcohol of **12** was converted to the corresponding

mesylate, which was subsequently displaced with sodium azide to give the *trans*-azido proline ester **16** in 88% yield over 2 steps. Hydrolysis of the methyl ester of **16** gave the proline acid **17**, which was then reacted with the tyrosine derivative **7** under standard HBTU coupling conditions to furnish the dipeptide **18** in 93% yield. Alternatively, dipeptide **18** is also accessible from the *cis*-alcohol **8** (from Scheme 1). Conveniently, mesylation and subsequent azide displacement of alcohol **8** proceeded smoothly to furnish product **18**, which was obtained without the necessity for chromatographic purification.
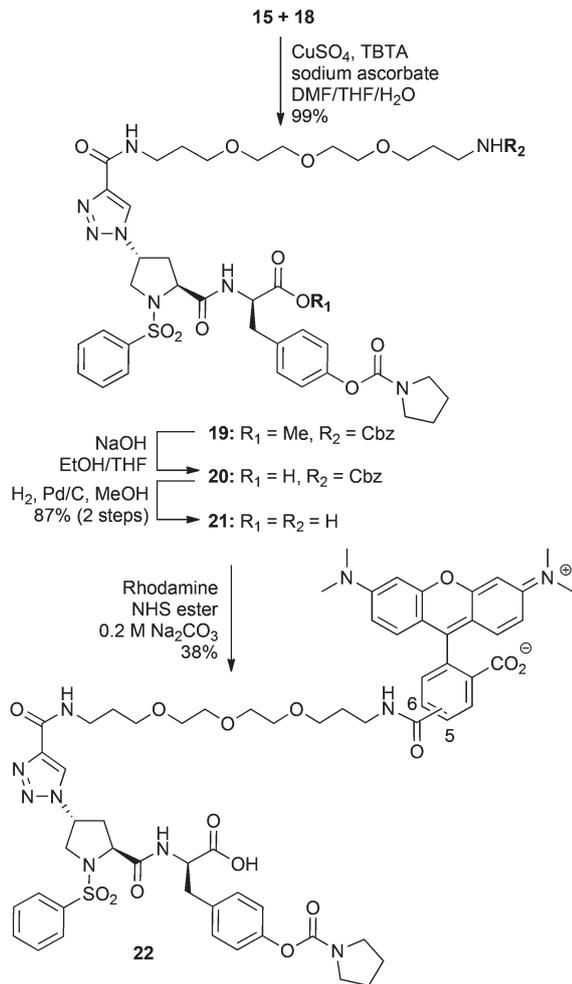
With the PEG alkyne **15** and azide **18** in hand, attention turned to their coupling using the CuAAC reaction (Scheme 4). Satisfyingly, treatment of **15** and **18** with $CuSO_4$, sodium ascorbate and the Cu(I)-stabilising ligand tris[(1-benzyl-1*H*-1,2,3-triazol-4-yl)methyl]amine (TBTA) gave the 1,4-disubstituted triazole **19** in virtually quantitative yield. Hydrolysis of methyl ester **19** gave the acid **20** and following removal of the Cbz group by hydrogenolysis, the fully deprotected PEG-functionalised integrin antagonist **21** was obtained in good yields (87% over 2 steps). Finally, treatment of amine **21** with NHS-rhodamine under aqueous conditions gave the fluorescent labelled integrin antagonist **22** in 38% yield as a 5:1 mixture of 5- and 6-carboxytetramethylrhodamine regioisomers after purification by C18 reversed phase chromatography.

Generally, it is appreciated that a sufficiently long spacer between the fluorophore and the bioactive molecule is required to prevent the fluorescent tag from interfering with small molecule–receptor interactions.[32] To assess the importance of linker length for this class of compounds, compound **25** (R-BC154), which lacks the PEG-spacer was also synthesised. Thus, hydrolysis of the methyl ester **18** with NaOH gave the deprotected azide inhibitor **23**, which was subsequently reacted with *N*-propynyl sulforhodamine B **24**[33] (ESI†) in the presence of $CuSO_4$, sodium ascorbate and TBTA
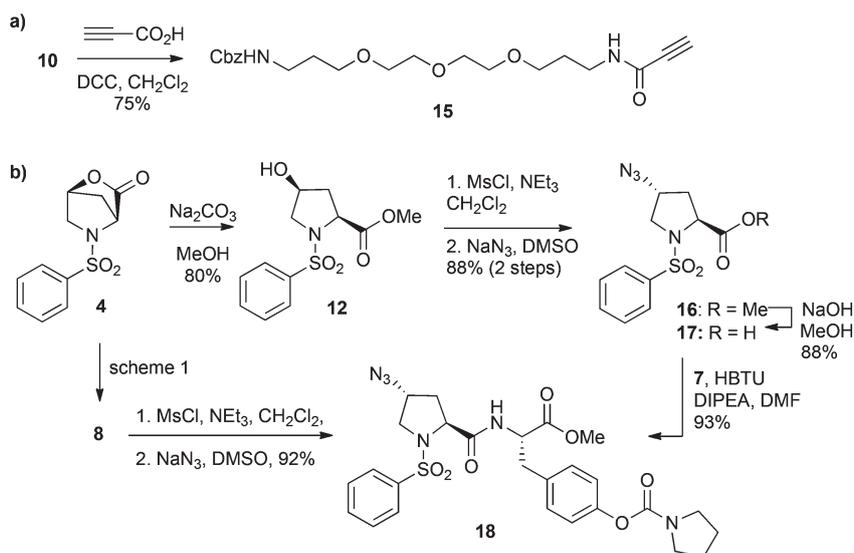
Scheme 3 Synthesis of (a) alkyne–functionalised PEG derivative **15** and (b) *trans*-azido *N*–phenylsulfonyl proline derivative **18**.
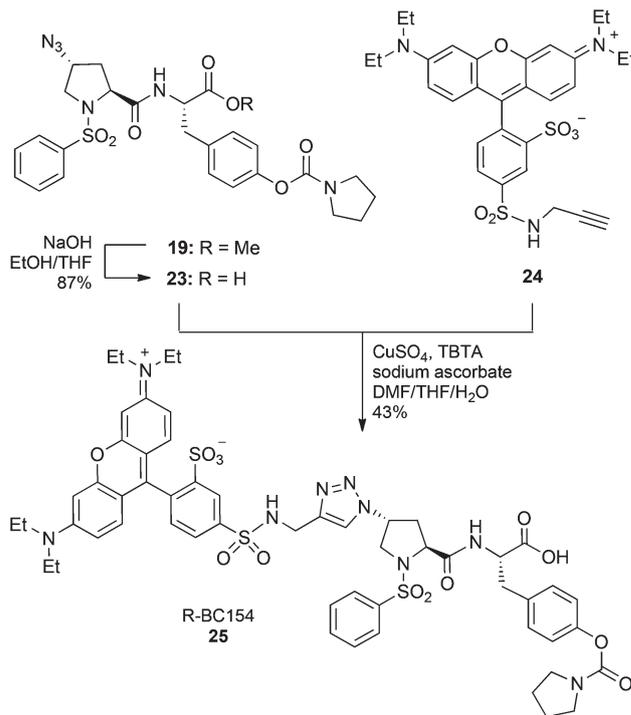
968 | *Org. Biomol. Chem.*, 2014, **12**, 965–978

This journal is © The Royal Society of Chemistry 2014

Scheme 4 Synthesis of 5(6)-carboxytetramethylrhodamine-labelled PEG-linked integrin antagonist **22**.

Scheme 5 Synthesis of lissamine rhodamine B-labelled integrin antagonist **25** (R–BC154).

to give the fluorescent labelled **25** (R-BC154) in 43% yield after purification by HPLC (Scheme 5).

In vitro binding properties of 22 and 25 (R-BC154) to $\alpha_4\beta_1$ and $\alpha_9\beta_1$ integrins

With fluorescent probes **22** and **25** (R-BC154) in hand, we assessed their integrin dependent cell binding properties using $\alpha_4\beta_1$ and $\alpha_9\beta_1$ over-expressing human glioblastoma LN18 cell lines that we generated (ESI Fig. S1 and S2†). When each LN18 cell line was treated with **22** and R-BC154 (**25**) under physiological mimicking conditions (1 mM Ca^{2+}/Mg^{2+}), both compounds were found to bind $\alpha_4\beta_1$ and $\alpha_9\beta_1$ LN18 cells in a dose-dependent manner (Fig. 3a and b). Virtually no binding was observed in the control cell line, which lacks integrin expression indicating that binding is integrin specific (Fig. 3a and b). Both the PEG-linked compound **22** and R-BC154 (**25**) bound $\alpha_9\beta_1$ integrin with greater selectivity than $\alpha_4\beta_1$ integrin as determined by their calculated dissociation constants (K_d). Specifically, compound **22** binds $\alpha_9\beta_1$ (K_d = 8.4 nM) with 2.4-fold greater affinity than $\alpha_4\beta_1$ (K_d = 20.1 nM) and R-BC154 has 3 times greater affinities for $\alpha_9\beta_1$ (K_d = 12.7 nM) relative to $\alpha_4\beta_1$

(K_d = 38.0 nM) under Ca^{2+}/Mg^{2+} conditions (Fig. 3a and b). Interestingly, when compared to compound **22**, R-BC154 was associated with only a 1.9-fold and 1.5-fold reduction in binding affinity to $\alpha_4\beta_1$ and $\alpha_9\beta_1$ integrins, respectively. These results suggest that both $\alpha_4\beta_1$ and $\alpha_9\beta_1$ integrins can indeed tolerate significant steric encumbrances at the 4-position of the proline residue for this class of *N*-phenylsulfonyl proline-based integrin antagonists. This observation indicates that there may be minimal benefits for the incorporation of a PEG linker. Nevertheless, while linkers separating the bioactive component from the fluorophore might not be necessary in this example, the incorporation of an amine-functionalised PEG linker (*e.g.* compound **21**) might find utility in other applications such as the functionalisation of surfaces, resins and microbeads for cell adherence, *ex vivo* culture and cell isolation purposes.[34,35]

The surprisingly high affinities of R-BC154 to $\alpha_4\beta_1/\alpha_9\beta_1$ integrins prompted us to explore its binding properties further. Like many integrin ligands, the affinity and binding kinetics of R-BC154 is also dependent on the activation state of integrins, which can be regulated by divalent metal cations.[36,37] As expected, no integrin binding was observed in the absence of cations (ESI Fig. S3†). However, in the presence of 1 mM Mn^{2+}, conditions known to induce integrins to adopt a higher affinity binding confirmation, we observed greater overall binding to both $\alpha_4\beta_1$ and $\alpha_9\beta_1$ over-expressing LN18 cell lines (Fig. 3b and c). Additionally, under Mn^{2+} activation a 3.1-fold increase in the binding affinity of R-BC154 towards $\alpha_4\beta_1$ (K_d = 12.4 nM) was observed when compared to Ca^{2+}/Mg^{2+}
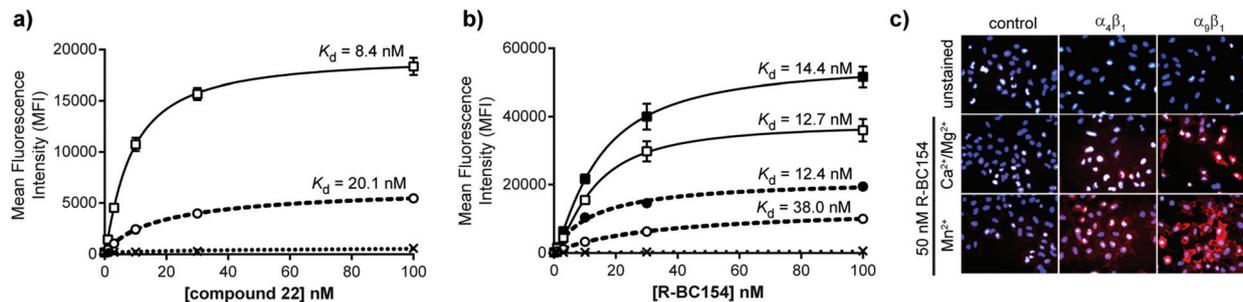
Fig. 3 Saturation binding experiment of compound **22** and R-BC154 to control (no integrins; cross-dotted line), $\alpha_4\beta_1$ (circle-dashed line) and $\alpha_9\beta_1$ (square-solid line) LN18 cells with (a) compound **22** in the presence of 1 mM Ca^{2+}/Mg^{2+} (open symbol) and (b) R-BC154 in the presence of either 1 mM Ca^{2+}/Mg^{2+} (open symbol) or 1 mM Mn^{2+} (closed symbol). Data shown are expressed as mean fluorescence intensity (MFI) $\pm$ SEM ($n = 3$). (c) Fluorescence microscopy images of over-expressing and control LN18 cells stained with 50 nM R-BC154 (red) under Ca^{2+}/Mg^{2+} and Mn^{2+} conditions. Cells were counterstained with DAPI (blue).
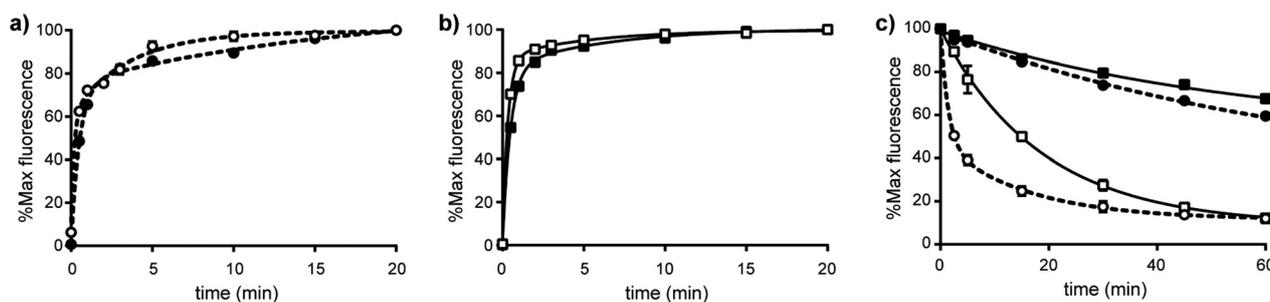

Fig. 4 Kinetics measurements of R-BC154 binding to LN18 cells. Association rates for binding of R-BC154 to (a) $\alpha_4\beta_1$ (circle-dashed line) and (b) $\alpha_9\beta_1$ (square-solid line) integrins were determined in the presence of 1 mM Ca^{2+}/Mg^{2+} (open symbol) and 1 mM Mn^{2+} (closed symbol) in TBS buffer by treatment of cells with 50 nM R-BC154 for 0, 0.5, 1, 2, 3, 5, 10, 15 and 20 minutes at 37 °C. (c) Dissociation rate measurements for binding of R-BC154 to $\alpha_4\beta_1$ (circle-dashed line) and $\alpha_9\beta_1$ (square-solid line) integrins were determined in the presence of 1 mM Ca^{2+}/Mg^{2+} (open symbol) and 1 mM Mn^{2+} (closed symbol) in TBS buffer at 0, 2.5, 5, 15, 30, 45 and 60 minutes. Data shown are expressed as % mean of maximum fluorescence $\pm$ SEM ($n = 3$) and plotted as a function of time. On-rate data were fitted to a two-phase association function for all curves ($R^2 > 0.997$). Off-rate data were fitted to a one-phase exponential decay function for all curves except $\alpha_4\beta_1$ (Ca^{2+}/Mg^{2+}), which was fitted to a two-phase exponential decay function ($R^2 > 0.999$).

conditions ($K_d = 38.0$ nM) (Fig. 3b). Despite the greater overall level of $\alpha_9\beta_1$ integrin binding that was induced by the addition of Mn^{2+}, a minimal change in the binding affinity was evident when compared to Ca^{2+}/Mg^{2+} conditions ($K_d = 14.4$ nM vs. 12.7 nM, respectively) (Fig. 3b).

The differences in the biochemical properties of $\alpha_4\beta_1$ and $\alpha_9\beta_1$ integrins were further investigated by measuring the kinetics of R-BC154 binding. Association rate measurements showed R-BC154 binding under Ca^{2+}/Mg^{2+} conditions was faster relative to Mn^{2+} conditions for both $\alpha_4\beta_1$ and $\alpha_9\beta_1$ integrins (Fig. 4a and b, respectively). Calculation of the on-rate constants (k_{on}) showed R-BC154 binding to $\alpha_4\beta_1$ integrin ($k_{on} = 0.094$ nM^{-1} min^{-1}) was faster than $\alpha_9\beta_1$ binding ($k_{on} = 0.061$ nM^{-1} min^{-1}) under physiological conditions (Table 1). Nevertheless, similar k_{on} values were observed under Mn^{2+} activation for both $\alpha_4\beta_1$ ($k_{on} = 0.038$ nM^{-1} min^{-1}) and $\alpha_9\beta_1$ integrins ($k_{on} \sim 0.04$ nM^{-1} min^{-1}) (Table 1).

The off-rate kinetics of R-BC154 binding was determined by dissociation experiments. Under both Ca^{2+}/Mg^{2+} and Mn^{2+} states, dissociation rates were faster for the R-BC154-$\alpha_4\beta_1$

complex ($k_{off} = 0.717$ and 0.014 min^{-1}) compared to its $\alpha_9\beta_1$ ($k_{off} = 0.054$ and <0.01 min^{-1}) counterpart (Fig. 4c and Table 1). In addition, the k_{off} values for R-BC154 binding to $\alpha_4\beta_1$ and $\alpha_9\beta_1$ integrins in the presence of Mn^{2+} was significantly slower compared to Ca^{2+}/Mg^{2+} conditions, with greater than 60% of R-BC154 still bound after 60 min (Fig. 4c). The slower off-rates observed under these conditions suggests Mn^{2+} acts to stabilise the ligand bound conformation and is consistent with previous reports using radiolabelled substrates.[12] Thus, while faster on-rates and off rates are observed with Ca^{2+}/Mg^{2+} conditions, Mn^{2+} activation is associated with slower on- and off-rates for $\alpha_4\beta_1$ and $\alpha_9\beta_1$ integrin binding. Consequently, competitive inhibition assays using R-BC154 for in vitro screening of small molecule integrin inhibitors under Ca^{2+}/Mg^{2+} conditions is preferred as the exceedingly slow off rates under Mn^{2+} activation would require much longer incubation times (data not shown). Our results suggest that although $\alpha_4\beta_1$ integrin binds slightly faster to this class of N-phenylsulfonyl proline-based antagonists compared to $\alpha_9\beta_1$, more prolonged binding is observed for $\alpha_9\beta_1$ integrin

970 | Org. Biomol. Chem., 2014, **12**, 965–978

This journal is © The Royal Society of Chemistry 2014

Table 1 Summary of R-BC154 binding properties to $\alpha_4\beta_1$ and $\alpha_9\beta_1$ over-expressing LN18 cells in the presence of Ca^{2+}/Mg^{2+} or Mn^{2+}

	Conditions	k_{obs}[a] (min^{-1})	k_{off}[b] (min^{-1})	k_{on}[e] (nM^{-1} min^{-1})
$\alpha_4\beta_1$ cells	1 mM Ca^{2+}/Mg^{2+}	5.426	0.717[c]	0.094
	1 mM Mn^{2+}	1.891	0.014	0.038
$\alpha_9\beta_1$ cells	1 mM Ca^{2+}/Mg^{2+}	3.117	0.054	0.061
	1 mM Mn^{2+}	2.035	<0.01[d]	~0.04

[a] The observed association rate (k_{obs}) represents the fast phase of binding and accounts for >60% and >80% of R-BC154 binding to $\alpha_4\beta_1$ and $\alpha_9\beta_1$ integrins, respectively. [b] Data from the dissociation experiment represented in Fig. 4c was fitted to a one-phase exponential decay function (unless otherwise stated) and dissociation rate constants (k_{off}) extrapolated from the curve. [c] Dissociation data for R-BC154 binding to $\alpha_4\beta_1$ LN18 cells in the presence of Ca^{2+}/Mg^{2+} was fitted to a two-phase dissociation curve and k_{off} was determined from the fast-phase of the curve, which accounted for >60% of the dissociation. [d] Dissociation of the R-BC154-$\alpha_9\beta_1$ integrin complex under Mn^{2+} activation was too slow (>55% still bound after 120 min; data not shown) to accurately calculate off-rates; k_{off} value was estimated based on an approximate half-life of ~100 min. [e] The association rate constant (k_{on}) was calculated using the formula (k_{obs} − k_{off})/[R-BC154 concentration = 50 nM].

(Table 1). Thus, under physiologically relevant conditions, this class of dual $\alpha_4\beta_1/\alpha_9\beta_1$ integrin inhibitors might be expected to elicit greater affects against $\alpha_9\beta_1$ integrin-dependent interactions *in vivo* owing to their significantly slower off-rates to $\alpha_9\beta_1$ despite the higher association rates observed for $\alpha_4\beta_1$ integrin.

In vivo binding of R-BC154 to bone marrow HSC and progenitor cells

Our *in vitro* binding data demonstrated that R-BC154 is a high affinity $\alpha_4\beta_1$ and $\alpha_9\beta_1$ integrin antagonist, whose binding activity is highly dependent on integrin activation. Thus, we speculated whether R-BC154 could be used in *in vivo* binding experiments to investigate $\alpha_4\beta_1/\alpha_9\beta_1$ integrin activity on defined populations of HSC. To date, assessing integrin activity on HSC has relied primarily on *in vitro* or *ex vivo* staining of bone marrow cells or purified HSC using fluorescent labelled antibodies. Whilst *ex vivo* staining provides confirmation of integrin expression by HSC, investigation of integrin activation in their native state within bone marrow can only be determined through *in vivo* binding experiments, as the complex bone marrow microenvironment cannot be adequately reconstructed *in vitro*.

To assess whether R-BC154 and this class of *N*-phenylsulfonyl proline-based peptidomimetics could bind directly to HSC, we injected R-BC154 (10 mg kg^{-1}) intravenously into mice and analysed R-BC154 labelling of phenotypically defined bone marrow progenitor cells (LSK cell; lineage$^-$Sca-1$^+$c-Kit$^+$) and HSC (LSKSLAM cell; LSKCD48$^-$CD150$^+$) using multi-colour flow cytometry (Fig. 5a and b). Increased cell-associated fluorescence as a result of R-BC154 binding was observed for both progenitor cells and HSC populations that were isolated from R-BC154 injected mice when compared to bone marrow from un-injected mice. Furthermore, *in vivo* R-BC154 binding was
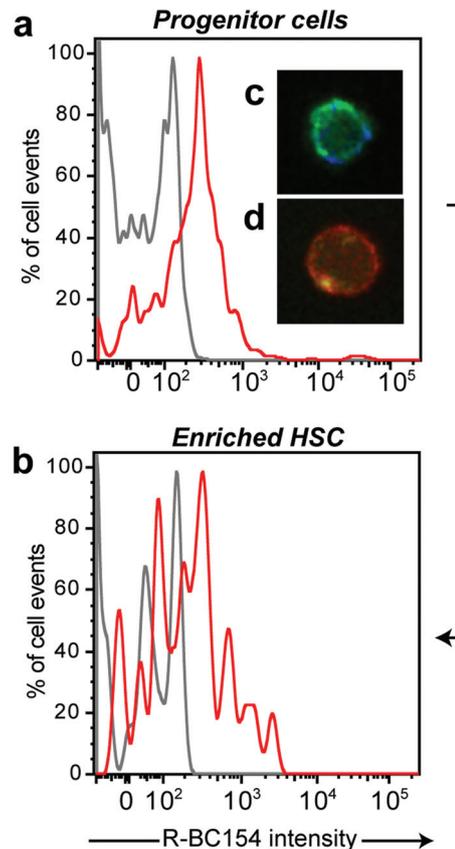

Fig. 5 Flow cytometric histogram plots of (a) bone marrow haemopoietic progenitor cells (LSK) and (b) HSC (LSKSLAM) isolated from untreated (grey lines) and R-BC154 (10 mg kg^{-1}) injected (red lines) C57Bl/6 mice. Data is representative of 3 biological samples. Fluorescent microscopy images (inset) of FACS sorted progenitor cells (Lineage$^-$Sca-1$^+$c-Kit$^+$) isolated from (c) untreated and (d) R-BC154 injected mice. Sca-1$^+$ (blue), c-Kit$^+$ (green), R-BC154$^+$ (red).

also confirmed by fluorescence microscopy on purified populations of progenitor cells (Lineage$^-$Sca-1$^+$c-Kit$^+$) (Fig. 5c and d). R-BC154 labelled progenitor cells exhibited a fluorescence halo indicating R-BC154 binding was primarily cell surface, which is consistent with integrin-binding. Our *in vivo* binding results indicate that this class of $\alpha_4\beta_1/\alpha_9\beta_1$ integrin antagonists are capable of binding to extremely rare populations of haemopoietic progenitor cells and HSC, which represent only 0.2% and 0.002% of mononucleated cells within murine bone marrow, respectively.[38]

The $\alpha_4\beta_1$ and $\alpha_9\beta_1$ integrins are recognised to be important modulators of HSC lodgement within bone marrow through binding to VCAM-1 and Opn.[18] Compound **2** has been shown to inhibit binding of $\alpha_4\beta_1$ and $\alpha_9\beta_1$ integrins to both VCAM-1 and Opn *in vitro* with nanomolar inhibitory potencies.[12] Our *in vivo* binding results using R-BC154 indicate that the $\alpha_4\beta_1$ and $\alpha_9\beta_1$ integrins expressed by HSC are in an active binding conformation *in situ*. This suggests that small molecule $\alpha_4\beta_1/\alpha_9\beta_1$ integrin antagonists such as **2**, not only bind directly to bone marrow HSC, but they might also be capable of inhibiting $\alpha_4\beta_1/\alpha_9\beta_1$ dependent adhesive interactions and potentially

This journal is © The Royal Society of Chemistry 2014

Org. Biomol. Chem., 2014, **12**, 965–978 | 971

serve as effective agents for inducing the mobilisation of bone marrow HSC into the peripheral circulation. Assessment of the HSC mobilisation properties of $\alpha_4\beta_1/\alpha_9\beta_1$ integrin antagonists in the context of peripheral blood stem cell transplants will be reported elsewhere.

Conclusion

In summary, we report the synthesis of two N-phenylsulfonyl proline-based fluorescent integrin antagonists, **22** and **25** (R-BC154), both exhibiting high nanomolar binding affinities to $\alpha_9\beta_1$ and $\alpha_4\beta_1$ integrins. Using the CuAAC reaction, we conjugated either an alkyne-functionalised PEG-linker or fluorophore to 4-azido N-phenylsulfonyl proline based peptidomimetics, which is a strategy that may also be applicable to other integrin inhibitors (*e.g.* $\alpha_2\beta_1$ antagonists) possessing similar proline derived scaffolds. By comparing the binding properties of **22** and R-BC154, we showed that a long linker separating the fluorophore from the bioactive component may not be significantly advantageous to integrin binding affinity or α_9/α_4 selectivity. Our *in vitro* binding kinetics experiments using R-BC154 demonstrated that this class of N-phenylsulfonyl proline-based inhibitors bind faster to $\alpha_4\beta_1$ integrin but exhibits more prolonged binding to $\alpha_9\beta_1$ integrin. Finally, we provide evidence that R-BC154 is capable of binding haemopoietic progenitor cells and HSC within mice bone marrow *in vivo*, indicating this class of inhibitors might be capable of inhibiting HSC dependent integrin interactions. Thus, R-BC154 is a useful high affinity, activation dependent integrin probe, which can be used to investigate $\alpha_9\beta_1$ and $\alpha_4\beta_1$ integrin binding activity both *in vitro* and *in vivo*.

Methods

General methods

All starting materials, reagents, and solvents were obtained from commercial sources and used without further purification unless otherwise stated. All anhydrous reactions were performed under a dry nitrogen atmosphere. Diethyl ether, dichloromethane, tetrahydrofuran and toluene were dried by passage through two sequential columns of activated neutral alumina on the Solvent Dispensing System built by J. C. Meyer and based on the original design by Grubbs and co-workers.[39] Petroleum spirits refers to the fraction boiling at 40–60 °C. Thin layer chromatography (TLC) was performed on Merck pre-coated 0.25 mm silica aluminium-backed plates and visualised with UV light and/or dipping in ninhydrin solution or phosphomolybdic acid solution followed by heating. Purification of reaction products was carried out by flash chromatography using Merck Silica Gel 60 (230–400 mesh) or reverse phase C18 silica gel. Melting points were recorded on a *Reichert-Jung* Thermovar *hot-stage* microscope melting point apparatus. Optical rotations were recorded on a Perkin Elmer Model 341 polarimeter. FTIR spectra were obtained using a

ThermoNicolet 6700 spectrometer using a SmartATR (attenuated total reflectance) attachment fitted with a diamond window. Proton (^{1}H) and carbon (^{13}C) NMR spectra were recorded on a BrukerAV400 spectrometer at 400 and 100 MHz, respectively. ^{1}H NMR are reported in ppm using a solvent as an internal standard (CDCl$_3$ at 7.26 ppm). Proton-decoupled ^{13}C NMR (100 MHz) are reported in ppm using a solvent as an internal standard (CDCl$_3$ at 77.16 ppm). High resolution mass spectrometry was acquired on either a WATERS QTOF II (CMSE, Clayton, VIC 3168) or a Finnigan hybrid LTQ-FT mass spectrometer (Thermo Electron Corp.) (Bio21 Institute, University of Melbourne, Parkville, VIC 3010) employing electrospray ionisation (ESI).

(1S,4S)-5-(Phenylsulfonyl)-2-oxa-5-azabicyclo[2.2.1]heptan-3-one (4). Diisopropylazocarboxylate (1.87 ml, 9.48 mmol) was added dropwise over 20 min to a stirred suspension of N-phenylsulfonyl-*trans*-4-hydroxy-L-proline (2.45 g, 9.03 mmol) and triphenylphosphine (2.49 g, 9.48 mmol) in CH$_2$Cl$_2$ (150 ml) at 0 °C under N$_2$. The reaction was warmed to rt and stirred overnight, concentrated under reduced pressure and the residue purified by flash chromatography (50 : 50 EtOAc–pet. spirits) to give the lactone **4** (1.77 g, 78%) as a colourless solid. Spectroscopic data is identical to previously reported values.[27]

(S)-4-(2-(((Benzyloxy)carbonyl)amino-3-methoxy-3-oxopropyl)-phenyl pyrrolidine-1-carboxylate (6). 1-Pyrrolidinecarbonyl chloride (336 μl, 3.04 mmol) was added to a Biotage™ microwave vial containing a mixture of the tyrosine **5** (500 mg, 1.52 mmol) and K$_2$CO$_3$ (420 mg, 3.04 mmol) in CH$_3$CN (9 ml). The mixture was heated to 100 °C in a microwave reactor for 45 min, diluted with H$_2$O and then stirred for 30 min. The aqueous layer was extracted with EtOAc (2 × 20 ml) and the combined organic phases washed with sat. aq. NaHCO$_3$, dried (MgSO$_4$) and concentrated under reduced pressure. The residue was recrystallised (EtOAc–pet. spirits) to give the carbamate **6** (484 mg, 75%) as colourless crystals, mp 116–117 °C; $[\alpha]_D$ +42.5 (c 0.81 in CHCl$_3$); δ_H (400 MHz, CDCl$_3$) 1.94 (4 H, m, (CH$_2$)$_2$), 3.09 (2 H, m), 3.47 (2 H, t, J = 6.5 Hz), 3.55 (2 H, t, J = 6.5 Hz), 3.71 (3 H, s), 4.64 (1 H, m), 5.10 (2 H, s), 5.22 (1 H, d, J = 8.0 Hz), 7.03–7.38 (9 H, m); δ_C (100 MHz, CDCl$_3$) 25.0, 25.8, 37.5, 46.3, 46.4, 52.3, 54.8, 67.00, 121.9 (2 C), 128.1 (2 C), 128.1, 128.5 (2 C), 130.0 (2 C), 132.4, 136.2, 150.6, 153.0, 155.6, 171.9; ν/cm^{-1} 3331, 2954, 1719, 1698; 1511, 1402, 1345, 1216, 1061, 1020, 866, 754, 699; HRMS (ESI$^+$) m/z 449.1686 (C$_{23}$H$_{26}$N$_2$NaO$_6$ [M + Na]$^+$ requires 449.1689).

(S)-4-(2-Amino-3-methoxy-3-oxopropyl)phenyl pyrrolidine-1-carboxylate (7). A mixture of protected tyrosine **6** (950 mg, 1.13 mmol) and Pd/C (10%, 50 mg) in MeOH (40 ml) was purged 3 times with H$_2$. The mixture was stirred under a H$_2$ atmosphere for 2 h at which point TLC indicated complete consumption of starting material. The mixture was filtered through a layer of Celite and the filtrate concentrated under reduced pressure to give the crude amine **7** (637 mg, 98%) as a colourless oil, which set solid upon standing. A small portion was further purified by flash chromatography (5 : 95 to 10 : 90 MeOH–CH$_2$Cl$_2$) for characterisation, $[\alpha]_D$ −11.6 (c 1.09 in

972 | *Org. Biomol. Chem.*, 2014, **12**, 965–978

This journal is © The Royal Society of Chemistry 2014

MeOH); δ_H (400 MHz, CDCl$_3$) 1.97 (4 H, m), 2.91 (1 H, dd, J = 7.1, 13.6 Hz), 3.02 (1 H, dd, J = 6.1, 13.6 Hz), 3.42 (2 H, t, J = 6.5 Hz), 3.43 (2 H, t, J = 6.5 Hz), 3.68 (3 H, s), 4.84 (2 H, br s), 3.70 (1 H, dd, J = 6.2, 7.1 Hz), 7.05 (2 H, m), 7.21 (2 H, m); δ_C (100 MHz, CDCl$_3$) 25.9, 26.7, 41.1, 47.5, 47.5, 52.4, 56.7, 123.0 (2 C), 131.2 (2 C), 135.6, 151.6, 155.1, 176.1; ν/cm^{-1} 3311, 2954, 2878, 1714, 1510, 1399, 1344, 1214, 1168, 1086, 1062, 1020, 864, 755; HRMS (ESI$^+$) m/z 293.1497 (C$_{15}$H$_{20}$N$_2$O$_4$SH [M + H]$^+$ requires 293.1496).

4-((S)-2-((2S,4S)-4-Hydroxy-1-(phenylsulfonyl)pyrrolidine-2-carboxamido)-3-methoxy-3-oxopropyl)phenyl pyrrolidine-1-carboxylate (8). The lactone **4** (466 mg, 1.84 mmol) and the amine **7** (510 mg, 1.76 mmol) in toluene–H$_2$O (5 : 1, 6 ml) was stirred at 80 °C for 2 d and then diluted with EtOAc and washed with 1 M HCl, sat. aq. NaHCO$_3$, brine, dried (MgSO$_4$) and concentrated under reduced pressure. The residue was purified by flash chromatography (100% EtOAc to 5% MeOH–EtOAc) to give the alcohol **8** (851 mg, 89%) as a colourless foam, $[\alpha]_D$ −31.4 (c 1.66 in MeOH); δ_H (400 MHz, CDCl$_3$) 1.57 (1 H, m), 1.89–2.00 (5 H, m), 2.94 (1 H, dd, J = 9.5, 14.0 Hz), 3.13 (1 H, dd, J = 4.0, 10.5 Hz), 3.23 (1 H, d, J = 10.5 Hz), 3.35 (1 H, dd, J = 5.0, 14.0 Hz), 3.40 (2 H, t, J = 6.5 Hz), 3.51–3.56 (3 H, m), 3.78 (3 H, s), 4.03 (1 H, m), 4.12 (1 H, d, J = 9.0 Hz), 4.75 (1 H, m), 6.99 (2 H, d, J = 8.3 Hz), 7.07 (1 H, d, J = 7.5 Hz), 7.19 (2 H, 8.3 Hz), 7.51–7.63 (3 H, m), 7.83 (2 H, d, J = 7.5 Hz); δ_C (100 MHz, CDCl$_3$) 25.1, 25.9, 37.0, 37.6, 46.5, 46.6, 52.6, 53.3, 57.8, 61.7, 69.7, 122.5 (2 C), 127.9 (2 C), 129.4 (2 C), 130.5 (2 C), 133.4, 133.8, 136.3, 150.2, 154.1, 171.6, 171.7; ν/cm^{-1} 3408, 1743, 1718, 1701, 1663; HRMS (ESI$^+$) m/z 568.1723 (C$_{26}$H$_{31}$NaN$_3$O$_8$S [M + Na]$^+$ requires 568.1730).

4-((R)-3-Methoxy-3-oxo-2-((2S,4R)-4-((3-oxo-1-phenyl-2,8,11,14-tetraoxa-4-azaheptadecan-17-yl)amino)-1-(phenylsulfonyl)pyrrolidine-2-carboxamido)propyl)phenyl pyrrolidine-1-carboxylate (11). Alcohol **8** (105 mg, 0.19 mmol) was dissolved in dry CH$_2$Cl$_2$ (2 ml) under N$_2$ at −20 °C. DIPEA (99 μl, 0.57 mmol) was added followed by Tf$_2$O (50 μl, 0.57 mmol) dropwise over 30 min. The reaction was stirred for 2 h at −20 °C and then quenched with sat. aq. NaHCO$_3$, diluted with EtOAc and the organic phase separated. The organic phase was washed with H$_2$O, 2% citric acid, sat. aq. NaHCO$_3$ and brine. The aqueous phase was extracted with EtOAc (2 times) and the combined organic phases dried (MgSO$_4$) and the residue concentrated under reduced pressure to give the crude triflate. To this residue was added the PEG amine **10** (141 mg, 0.39 mmol) in dry THF (200 μl) and the reaction stirred overnight at rt. The mixture was diluted with 10% butan-2-ol–EtOAc (20 ml) and the organic phase washed with sat. aq. NaHCO$_3$, brine, dried (MgSO$_4$) and concentrated under reduced pressure. The crude residue was purified by flash chromatography (2% to 3% MeOH–CH$_2$Cl$_2$) to give **11** (46 mg, 27% over 2 steps) as a colourless oil. A small portion was further purified by C18-silica gel chromatography (40% H$_2$O–MeCN) for characterisation, δ_H (400 MHz, CDCl$_3$) 1.40 (1H, m), 1.55 (2H, m), 1.77 (2H, m), 1.93 (4H, m), 2.12 (1H, m), 2.43 (2H, m), 2.82 (1H, dd, J = 7.8, 9.2 Hz), 2.94 (1 H, m), 3.02 (1 H, dd, J = 7.8, 14.0 Hz), 3.23–3.32 (4 H, m), 3.38 (2H, t, J = 6.1 Hz), 3.44 (2H, t, J = 6.6 Hz), 3.46–3.60 (14H, m), 3.76 (3H, s), 4.09 (1H, dd, J = 3.0, 8.9 Hz), 4.85 (1H, td, J = 5.7, 7.8 Hz), 5.07 (2H, s), 5.42 (1H, brs), 7.05 (2H, d, J = 8.6 Hz), 7.14 (2H, d, J = 8.6 Hz), 7.21 (1H, d, J = 7.8 Hz), 7.28–7.35 (5H, br m), 7.53 (2H, t, J = 7.5 Hz), 7.60 (1H, br t, J = 7.04), 7.81 (1H, br d, J = 7.05 Hz); δ_C (100 MHz, CDCl$_3$) 25.1, 25.9, 29.6, 30.1, 36.5, 37.5, 39.4, 45.9, 46.5, 46.6, 52.6, 53.3, 54.7, 56.5, 61.6, 66.6, 69.8, 69.7, 70.3, 70.3, 70.67, 70.72, 122.0 (2 C), 128.1 (2 C), 128.2 (2 C), 128.6 (3 C), 129.4 (2 C), 130.2 (2 C), 133.0, 133.5, 136.0, 137.0, 150.7, 153.2, 156.6, 170.9, 171.6; ν/cm^{-1} 3334, 2877, 2341, 1706, 1521. HRMS (ESI$^+$) m/z 904.3770 (C$_{44}$H$_{59}$NaN$_5$O$_{12}$S [M + Na]$^+$ requires 904.3779).

Methyl (2S,4S)-4-hydroxy-1-(phenylsulfonyl)pyrrolidine-2-carboxylate (12). A mixture of lactone **4** (1.74 g, 6.88 mmol) and Na$_2$CO$_3$ (3.65 g, 34.4 mmol) was stirred in MeOH (50 ml) at rt overnight. The residue was concentrated, taken up in EtOAc (100 ml), and H$_2$O and the organic phase separated. The aqueous phase was extracted with EtOAc (2 × 30 ml) and the combined organic phases washed with brine, dried (MgSO$_4$) and concentrated under reduced pressure to give the methyl ester **12** (1.57 g, 80%) as a colourless solid. Spectroscopic data is consistent with reported values and the material was used without further purification.[27]

(2S,4R)-Methyl-4-((3-oxo-1-phenyl-2,8,11,14-tetraoxa-4-azaheptadecan-17-yl)amino)-1-(phenylsulfonyl)-pyrrolidine-2-carboxylate (13). Proline ester **12** (100 mg, 0.35 mmol) was dissolved in dry CH$_2$Cl$_2$ (1 ml) under N$_2$ at −20 °C. DIPEA (192 μl, 0.53 mmol) was added followed by Tf$_2$O (89 μl, 0.53 mmol) dropwise over 10 min. The mixture was stirred at −20 °C for 2 h and then PEG amine **10** (248 mg, 0.70 mmol) in CH$_2$Cl$_2$ (3 ml) was added dropwise at −20 °C. The reaction was stirred for 1 h at −20 °C and then warmed to rt for 4 h. Saturated NaHCO$_3$ and EtOAc were added and the reaction mixture extracted, washed with water, dried over MgSO$_4$ and the solvent removed under reduced pressure. The crude material was purified by flash chromatography (100% CH$_2$Cl$_2$ then 5% MeOH–CH$_2$Cl$_2$ with 1% NEt$_3$) to give **13** as a pale yellow oil (319 mg, 30%), δ_H (200 MHz, CDCl$_3$) 1.62 (1H, br t, J = 4.0 Hz), 1.75–1.85 (4H, m), 1.95–2.05 (1H, m), 2.12–2.21 (1H, m), 2.59 (2H, br s), 3.17 (1H, br s), 3.31 (2H, q, J = 6.3 Hz), 3.42 (1H, t, J = 5.7 Hz), 3.45–3.69 (13H, m), 3.70 (3H, s), 4.37 (1H, dd, J = 5.7, 8.7 Hz), 5.08 (2H, s), 5.40 (1H, br s), 7.27–7.38 (5H, m), 7.52 (2H, t, J = 7.5), 7.57–7.60 (1H, m), 7.84–7.89 (2H, m); δ_C (100 MHz, CDCl$_3$) 29.5, 29.7, 37.0, 39.3, 45.7, 52.6, 53.4, 56.9, 59.6, 66.6, 69.7, 69.7, 70.2 (2 C), 70.60, 70.62, 127.7 (2 C), 128.1 (2 C), 128.2, 128.6 (2 C), 129.1 (2 C), 133.0, 136.9, 138.0, 156.6, 172.5; ν/cm^{-1} 3400, 3300, 2980, 2925, 2868, 1787, 1710, 1526; HRMS (EI$^+$) m/z 622.2795 (C$_{30}$H$_{43}$N$_3$O$_9$SH [M + H]$^+$ requires 622.2798).

Methyl (S)-4-oxo-1-(phenylsulfonyl)pyrrolidine-2-carboxylate (14). A mixture of proline ester **12** (300 mg, 1.05 mmol) and PCC (907 mg, 4.2 mmol) in dry CH$_2$Cl$_2$ (20 ml) was stirred for 2 d at rt. The mixture was filtered through a plug of silica and the solvent removed under reduced pressure to obtain the ketone **14** (260 mg, 88%) as colourless crystals, mp 89.5–90.3 °C (lit[40] 83.5–84.5 °C); δ_H (200 MHz, CDCl$_3$) 2.56

(1H, dd, J = 3.0 18.2 Hz), 2.82 (1H, dd, J = 9.3, 18.2 Hz), 3.59 (3H, s), 3.76 (1H, d, J = 17.4 Hz), 3.90 (1H, d, J = 17.4 Hz), 4.81 (1H, dd, J = 3.0, 9.3 Hz), 7.50–7.70 (3H, m), 7.81–7.90 (2H, m); δ_C (75 MHz, CDCl$_3$) 41.7, 52.8, 52.9, 57.6, 127.6, 129.6, 133.7, 137.7, 170.8, 206.2; ν/cm^{-1} 3002, 2961, 1763, 1747; HRMS (EI$^+$) m/z 306.0412 (C$_{12}$H$_{13}$NO$_5$SNa [M + Na]$^+$ requires 306.0412).

Reductive amination method

The PEG amine **10** (189 mg, 0.53 mmol) was added to a solution of the ketone **14** (150 mg, 0.53 mmol) in dry CH$_2$Cl$_2$ (2 ml) under N$_2$. Na(OAc)$_3$BH (156 mg, 0.74 mmol) was added, followed by acetic acid (30 μl, 0.53 mmol) and the reaction stirred for 24 h at rt. Additional Na(OAc)$_3$BH (0.5 eq.) was added and the reaction stirred for a further 24 h. The reaction was quenched with NaOH (1 M) and extracted with CH$_2$Cl$_2$, washed with H$_2$O, dried and the solvent removed under reduced pressure. The crude material was purified by flash chromatography (CH$_2$Cl$_2$ to 5% MeOH–CH$_2$Cl$_2$ with 1% NEt$_3$) to give **13** (99 mg, 30%) as a 2 : 1 mixture of *cis* : *trans* diastereoisomers.

Benzyl (15-oxo-4,7,10-trioxa-14-azaheptadec-16-yn-1-yl)carbamate (15). Diisopropylcarbodiimide (291 μl, 1.86 mmol) was added to a mixture of PEG amine **10** (0.55 g, 1.55 mmol) and propiolic acid (96 μl, 1.55 mmol) in dry CH$_2$Cl$_2$ (5 ml) at 0 °C. The reaction was warmed to rt and stirred for 2 h and then concentrated. The residue was taken up in EtOAc and the urea byproduct precipitate removed by filtration through a layer of celite filtered off through a layer of celite to remove the urea byproduct. The organic filtrate was concentrated under reduced pressure and the residue purified by flash chromatography (80% EtOAc–pet. spirits to 100% EtOAc to 5% MeOH–EtOAc) to give the alkyne **12** (472 mg, 75%) as a colourless oil, δ_H (400 MHz, CDCl$_3$) major rotamer: 1.76 (4 H, m), 2.74 (1 H, s), 3.31 (2 H, dd, J = 6.1, 12.3 Hz), 3.39 (2 H, dd, J = 5.9, 12.3 Hz), 3.51–3.64 (12 H, m), 5.08 (2 H, br s), 5.34 (1 H, br s), 6.82 (1 H, br s), 7.27–7.35 (5 H, m); δ_C (100 MHz, CDCl$_3$) major rotamer; 23.6, 28.6, 38.6, 39.5, 66.6, 69.8. 70.1, 70.3 (2 C), 70.6, 70.7 (2 C), 72.7, 128.2, 128.3, 128.6 (3 C), 136.9, 152.2, 156.6; ν/cm^{-1} 3292, 2924, 2871, 2105, 1704, 1645, 1535; HRMS (ESI$^+$) m/z 407.2177 (C$_{21}$H$_{31}$N$_2$O$_6$Na [M + Na]$^+$ requires 407.2182).

Methyl (2S,4R)-4-azido-1-(phenylsulfonyl)pyrrolidine-2-carboxylate (16). MsCl (304 μl, 3.93 mmol) was added to a mixture of the alcohol **12** (934 mg, 3.27 mmol) and triethylamine (620 μl, 4.48 mmol) in dry CH$_2$Cl$_2$ (20 ml) at 0 °C under N$_2$. The mixture was stirred for 2 h, diluted with CH$_2$Cl$_2$ and washed sequentially with 5% HCl, sat. aq. NaHCO$_3$, brine, dried (MgSO$_4$) and concentrated under reduced pressure to give the crude mesylate as a pale yellow oil. This residue was taken up in DMSO (13 ml) and treated with NaN$_3$ (638 mg, 9.81 mmol) and the mixture stirred overnight at 80 °C. The reaction was diluted with EtOAc and washed with H$_2$O, brine, dried (MgSO$_4$) and concentrated. The residue was purified by recrystallisation (MeOH) to give **16** (874 mg, 86% over 2 steps) as colourless needles, mp 98–100 °C, [α]$_D$ −33.4 (c 1.02 in CHCl$_3$); δ_H (400 MHz, CDCl$_3$) 2.17–2.21 (2 H, m), 3.43 (1 H,

ddd, J = 0.7, 3.0, 11.0 Hz), 3.71 (1 H, dd, J = 5.0, 11.0 Hz), 3.76 (3 H, s), 4.18–4.22 (1 H, m), 4.30 (1 H, t, J = 7.5 Hz), 7.53–7.58 (2 H, m), 7.61–7.65 (1 H, m), 7.87–7.89 (2 H, m); δ_C (100 MHz, CDCl$_3$) 36.5, 52.9, 53.2, 59.45, 59.51, 127.6 (2 C), 129.3 (2 C), 133.3, 137.6, 171.9; ν/cm^{-1} 2101, 1747, 1445, 1345, 1207, 1158, 1095, 1017, 758, 722, 696; HRMS (ESI$^+$) m/z 311.0808 (C$_{12}$H$_{14}$N$_4$O$_4$SH [M + H]$^+$ requires 311.0809); m/z 328.1073 (C$_{12}$H$_{14}$N$_4$O$_4$SNH$_4$ [M + NH$_4$]$^+$ requires 328.1074).

(2S,4R)-4-Azido-1-(phenylsulfonyl)pyrrolidine-2-carboxylic acid (17). The methyl ester **16** (586 mg, 1.89 mmol) in 3 : 1 EtOH–THF (40 ml) was treated with 0.2 M NaOH (12.3 ml, 2.45 mmol). The mixture was stirred for 3 h at rt and then concentrated under reduced pressure. The crude material was diluted with ether and the aqueous phase separated. The organic layer was extracted with 0.2 M NaOH (2 × 10 ml) and the combined aqueous extract was acidified with 10% HCl. The aqueous layer was extracted with CHCl$_3$ (4 × 30 ml) and the combined organic phases washed with brine, dried (MgSO$_4$) and concentrated under reduced pressure. The crude material was purified by flash chromatography (5% MeOH–CH$_2$Cl$_2$ with 0.5% AcOH) to give acid **17** (492 mg, 88%) as a colourless oil, [α]$_D$ −34.4 (c 0.82 in MeOH); δ_H (400 MHz, CDCl$_3$) 2.18–2.32 (2 H, m), 3.40 (1 H, m), 3.73 (1 H, dd, J = 4.8, 11.5 Hz, H5′), 4.22 (1 H, m, H4) 4.29 (1 H, t, J = 7.7 Hz), 7.56 (2 H, m), 7.64 (1 H, m), 7.88 (2 H, m), 10.72 (1 H, br s); δ_C (100 MHz, CDCl$_3$) 36.1, 53.4, 59.5, 127.6 (2 C), 129.4 (2 C), 133.6, 136.9, 176.6; ν/cm^{-1} 3500–2500, 2107, 1731; HRMS (ESI$^+$) m/z 319.0472 (C$_{11}$H$_{12}$N$_4$NaO$_4$S [M + Na]$^+$ requires 319.0472).

4-(((S)-2-((2S,4R)-4-Azido-1-(phenylsulfonyl)pyrrolidine-2-carboxamido)-3-methoxy-3-oxopropyl)phenyl pyrrolidine-1-carboxylate (18). *O*-(Benzotriazol-1-yl)-*N*,*N*,*N′*,*N′*-tetramethyl uronium hexafluorophosphate (HBTU) (693 mg, 1.83 mmol) was added to a stirred mixture of acid **17** (491 mg, 1.66 mmol) and *N*,*N*-diisopropylethylamine (DIPEA) (578 μl, 3.32 mmol) in DMF (6 ml) at 0 °C and stirred for 10 min under N$_2$. Amine **7** (484 mg, 1.66 mmol) in DMF (6 ml) was then added dropwise and the combined mixture warmed to rt and stirred overnight. The mixture was diluted with EtOAc, washed sequentially with 5% HCl, sat. aq. NaHCO$_3$, brine, dried (MgSO$_4$) and concentrated under reduced pressure. The residue was purified by flash chromatography (3% MeOH–CH$_2$Cl$_2$) to give the dipeptide **7** (928 mg, 98%) as a pale yellow foam, [α]$_D$ −4.6 (c 0.85 in CHCl$_3$); δ_H (400 MHz, CDCl$_3$) 1.67 (1 H, m), 1.86–1.98 (4 H, m), 2.04 (1 H, dt, J = 5.5, 13.2 Hz), 2.99 (1 H, dd, J = 8.5, 14.0 Hz), 3.19 (1 H, dd, J = 4.5, 10.9 Hz), 3.30 (1 H, dd, J = 5.5 14.0 Hz), 3.44 (2 H, t, J = 6.5 Hz), 3.48 (1 H, dd, J = 5.5, 11.5 Hz), 3.53 (2 H, t, J = 6.5 Hz), 3.78 (3 H, s), 3.82 (1 H, m), 4.09 (1 H, dd, J = 5.5, 8.4 Hz), 4.87 (1H, dt, J = 8.3, 8.3, 5.5 Hz), 7.05, 7.15 (4 H, 2 × d, J = 8.5 Hz), 7.19 (1 H, d, J = 8.2 Hz), 7.53–7.57 (2 H, m), 7.62–7.66 (1 H, m), 7.83–7.86 (2 H, m); δ_C (100 MHz, CDCl$_3$) 25.1, 25.9, 35.6, 37.5, 46.4, 46.6, 52.7, 53.1, 53.8, 58.9, 61.1, 122.1 (2 C), 128.0 (2 C), 129.5 (2 C), 130.2 (2 C), 132.9, 133.7, 136.0, 150.7, 153.1, 169.9, 171.5; ν/cm^{-1} 3316, 2975, 2880, 2105, 1716, 1682; HRMS (ESI$^+$) m/z 593.1789 (C$_{26}$H$_{30}$N$_6$NaO$_7$S [M + Na]$^+$ requires 593.1789).

Synthesis of 18 *via* alcohol 8

Methanesulfonyl chloride (92 μl, 1.18 mmol) was added to a stirred mixture of the alcohol **8** (251 mg, 0.394 mmol) and triethylamine (170 ml, 1.22 mmol) in dry CH_2Cl_2 at 0 °C under N_2. The reaction was stirred for 1 h at 0 °C and then warmed to rt and stirred for a further 1 h. The reaction was diluted with CH_2Cl_2 and washed sequentially with 5% HCl, sat. aq. $NaHCO_3$ and brine. The organic phase was dried ($MgSO_4$) and concentrated under reduced pressure to give the intermediate mesylate (4-((*S*)-3-methoxy-2-((2*S*,4*S*)-4-((methylsulfonyl)oxy)-1-(phenylsulfonyl)pyrrolidine-2-carboxamido-3-oxopropyl)phenyl pyrrolidine-1-carboxylate) (270 mg, quant) as a colourless foam, which was used without further purification, $[\alpha]_D$ −13.5 (*c* 1.0 in $CHCl_3$); δ_H (400 MHz, $CDCl_3$) 1.81 (1 H, m), 1.89–1.96 (4 H, m), 2.63 (1 H, br d), 2.82 (3 H, s), 3.06–3.18 (2 H, m), 3.44 (2 H, t, *J* = 6.4 Hz), 3.50–3.55 (3 H, m), 3.68 (1 H, dt, *J* = 1.3, 12.5 Hz), 3.71 (3 H, s), 4.63 (1 H, dd, *J* = 2.0, 10.1 Hz), 4.73 (1 H, dd, *J* = 6.7, 13.4 Hz), 5.02 (1 H, tt, *J* = 1.4, 4.7 Hz), 7.07 (2 H, d, *J* = 8.6), 7.16 (2 H, d, *J* = 8.6 Hz), 7.39 (1 H, d, *J* = 7.5 Hz), 7.56 (2 H, t, *J* = 7.6 Hz), 7.64–7.68 (1 H, m), 7.81–7.84 (2 H, m); δ_C (100 MHz, $CDCl_3$) 25.1, 25.9, 35.5, 37.4, 38.9, 46.5, 46.5, 52.5, 54.0, 55.4, 61.0, 78.0, 122.1 (2 C), 128.0 (2 C), 129.8 (2 C), 130.1 (2 C), 132.8, 134.1, 135.4, 150.7, 153.1, 169.8, 171.3; ν/cm^{-1} 3409, 2954, 2880, 1715, 1678, 1511; HRMS (ESI$^+$) *m/z* 646.1497 ($C_{27}H_{33}NaN_3O_{10}S_2$ [M + Na]$^+$ requires 646.1505).

The above mesylate (97 mg, 0.16 mmol) was taken up in DMSO (1.5 ml) and treated with NaN_3 (30.4 mg, 0.47 mmol) and the mixture stirred overnight at 80 °C. The reaction was diluted with EtOAc and washed with H_2O, brine, dried ($MgSO_4$) and concentrated to give azide **18** (82 mg, 92%). Spectroscopic data were consistent with those reported above.

4-((*R*)-3-Methoxy-3-oxo-2-((2*S*,4*R*)-4-(4-((3-oxo-1-phenyl-2,8,11,14-tetraoxa-4-azaheptadecan-17-yl)carbamoyl)-1*H*-1,2,3-triazol-1-yl)-1-(phenylsulfonyl)pyrrolidine-2-carboxamido)propyl)phenyl pyrrolidine-1-carboxylate (19).

Sodium ascorbate (4.4 mg, 22.2 μmol), $CuSO_4$ (224 μl, 2.24 μmol, 0.01 M in H_2O) and TBTA (281 μl, 2.81 μmol, 0.01 M in THF) were added sequentially to a mixture of the azide **18** (32 mg, 56.1 μmol) and the alkyne **15** (25 mg, 61.8 μmol) in DMF (1 ml). The reaction was stirred at 60 °C for 2 h and then diluted with EtOAc (20 ml). The organic phase was washed with sat. aq. $NaHCO_3$, brine, dried ($MgSO_4$) and concentrated under reduced pressure. The residue was purified by flash chromatography (21 : 2 : 1 : 1 EtOAc–acetone–MeOH–H_2O) to give the triazole product **19** (54 mg, 99%) as a colourless oil, $[\alpha]_D$ +10.7 (*c* 1.0 in $CHCl_3$); δ_H (400 MHz, $CDCl_3$) 1.72–1.94 (8 H, m), 2.14 (1 H, dt, *J* = 12.8, 13.9 Hz), 2.54 (1 H, ddd, *J* = 2.3, 6.5, 12.9 Hz), 2.92 (1 H, dd, *J* = 10.0, 13.9 Hz), 3.29 (2 H, dd, *J* = 6.0, 12.3 Hz), 3.38 (1 H, dd, *J* = 4.8, 13.9 Hz), 3.41–3.63 (19 H, m), 3.80 (3 H, s), 3.83 (1 H, m), 4.29 (1 H, dd, *J* = 2.0, 8.7 Hz), 4.65 (1 H, m), 4.94 (1 H, dt, *J* = 4.9, 9.8 Hz), 5.06 (2 H, br s), 5.44 (1 H, br t, *J* = 5.7 Hz), 7.04 (2 H, d, *J* = 8.5 Hz), 7.23 (2 H, d, *J* = 8.5 Hz), 7.28–7.33 (5 H, m), 7.38–7.43 (2 H, m), 7.52 (2 H, t, *J* = 7.7 Hz), 7.62 (1 H, t, *J* = 7.5 Hz), 7.79 (2 H, d, *J* = 7.3 Hz), 8.18 (1 H, s); δ_C (100 MHz, $CDCl_3$) 25.1, 25.9, 29.4, 29.5, 33.7, 37.2, 37.9, 39.4, 46.4, 46.6, 52.7, 53.2,

53.6, 57.9, 60.7, 66.5, 69.7, 69.7, 70.3, 70.5, 70.6, 70.7, 122.2 (2 C), 126.1, 127.7 (2 C), 128.1, 128.2, 128.5 (3 C), 129.7 (2 C), 130.3 (2 C), 133.1, 133.9, 135.5, 136.9, 143.2, 150.6, 153.3, 156.6, 159.8, 169.0, 171.5; ν/cm^{-1} 3331, 2951, 2875, 1714, 1667, 1575, 1512; HRMS (ESI$^+$) *m/z* 999.3891 ($C_{47}H_{60}NaN_8O_{13}S$ [M + Na]$^+$ requires 999.3893).

(*R*)-2-((2*S*,4*R*)-4-(4-((3-(2-(2-(3-Aminopropoxy)ethoxy)ethoxy)propyl)carbamoyl)-1*H*-1,2,3-triazol-1-yl)-1-(phenylsulfonyl)pyrrolidine-2-carboxamido)-3-(4-((pyrrolidine-1-carbonyl)oxy)phenyl)propanoic acid (21).

$NaOH_{aq}$ (1.13 ml, 0.225 mmol, 0.2 M) was added to a stirred mixture of methyl ester **19** (110 mg, 0.113 mmol) in EtOH–THF (2 : 1, 3 ml) and stirred overnight at rt. The reaction was quenched with 1 M HCl, diluted with EtOAc and the organic phase separated. The aqueous phase was extracted twice with $CHCl_3$ and the combined organic phases dried ($MgSO_4$) and concentrated under reduced pressure to give the crude acid **20** (100 mg). A mixture of the crude acid and 10% Pd/C (50 mg, 50% H_2O) in MeOH–H_2O (5 : 1, 12 ml) was stirred under a H_2 atmosphere for 2 h at rt. The mixture was filtered through a layer of Celite, concentrated under reduced pressure and the residue purified using a C18 reversed phase cartridge (100% H_2O to 50% MeOH–H_2O). The purified material was lyophilised to give the amine **21** (81.3 mg, 87% over 2 steps) as a colourless fluffy powder, $[\alpha]_D$ −16.0 (*c* 0.49 in MeOH); δ_H (400 MHz, D_2O) 1.81 (4 H, m), 1.91 (4 H, m), 2.38 (1 H, m), 2.98–3.09 (4 H, m), 3.21–3.30 (3 H, m), 3.30 (2 H, m), 3.45 (2 H, t, *J* = 6.8 Hz), 3.59–3.66 (12 H, m), 3.89 (1 H, d, *J* = 12.9 Hz), 4.04 (1 H, dd, *J* = 4.8, 12.9 Hz), 4.41 (1 H, t, *J* = 8.2 Hz), 4.53 (1 H, dd, *J* = 5.3, 7.4 Hz), 5.00 (1 H, br s), 6.99 (2 H, d, *J* = 8.5 Hz), 7.306–7.356 (4 H, m), 7.43–7.50 (3 H, m), 7.99 (1 H, s); δ_C (100 MHz, D_2O with acetone) 25.2, 25.8, 27.2, 29.1, 35.5, 36.9, 37.2, 38.3, 47.1, 47.1, 49.5, 55.1, 56.7, 60.4, 61.7, 68.9, 69.3, 70.1, 70.2, 70.3, 122.6 (2 C), 125.8, 127.5 (2 C), 130.2 (2 C), 131.2 (2 C), 134.5, 135.1, 135.6, 142.9, 150.4, 155.6, 161.9, 173.2, 175.8; ν/cm^{-1} 3382, 3064, 2950, 2878, 1706, 1658, 1511; HRMS (ESI$^+$) *m/z* 829.3550 ($C_{38}H_{52}N_8O_{11}S$ [M + H]$^+$ requires 829.3549).

5(6)-Carboxytetramethyl rhodamine labelled compound (22).

A mixture of the amine **21** (9.5 mg, 11.3 μmol) in 0.2 M $NaHCO_3$ (1 ml) was treated with 5(6)-carboxytetramethyl rhodamine *N*-succinimidyl ester (NHS-rhodamine, Thermo Scientific) (8.9 mg, 16.9 μmol) and the mixture overnight at rt. The reaction was quenched with acetic acid, concentrated and the residue purified by reversed phase chromatography (50% MeOH–H_2O to 100% MeOH) to give the rhodamine labelled compound **22** (5.3 mg, 38%) as a purple powder after lyophilisation. Compound **22** was isolated as a 5 : 1 mixture of regioisomers; δ_H (400 MHz, d_4-methanol) major isomer: 1.80–1.99 (9 H, m), 2.37 (1 H, dt, *J* = 6.6, 13.5 Hz), 2.70 (1 H, m), 3.08 (1 H, dd, *J* = 7.5, 13.9 Hz), 3.22–3.26 (1 H, m), 3.26 (6 H, s), 3.27 (6 H, s), 3.35 (2H, t, *J* = 6.3 Hz), 3.43 (2H, t, *J* = 6.3 Hz), 3.48–3.66 (17 H, m), 3.74 (1 H, dd, *J* = 3.7, 12.0 Hz), 3.91 (1 H, dd, *J* = 6.0, 12.0 Hz), 4.45 (1 H, t, *J* = 7.1 Hz), 4.61 (1 H, t, *J* = 5.6 Hz), 4.94 (1 H, m), 6.86 (2 H, br s), 6.95–6.99 (4 H, m), 7.16 (2 H, d, *J* = 9.5 Hz), 7.28 (2 H, d, *J* = 8.1 Hz), 7.35–7.42 (3 H, m), 7.51 (1 H, t, *J* = 7.3 Hz), 7.60–7.63 (2 H, m), 8.06–8.08 (2 H, m),

This journal is © The Royal Society of Chemistry 2014

Org. Biomol. Chem., 2014, **12**, 965–978 | **975**

8.56 (1 H, s); δ_C (100 MHz, d_4-methanol) major isomer: 25.9, 26.7, 30.4, 36.6, 38.0, 38.1, 38.9, 40.9 (4 C), 47.47, 47.53, 55.9, 60.3, 62.3, 70.3, 70.5, 71.35, 71.4, 71.6 (2 C), 97.3 (2 C), 114.8 (2 C), 115.2 (2 C), 122.7 (4 C), 126.3, 128.6 (2 C), 130.0, 130.1, 130.5 (2 C), 131.1, 131.7 (4 C), 132.5 (2 C), 134.4 (2 C), 136.0, 137.2, 137.3, 138.1, 144.0, 151.6, 155.1, 158.7 (2 C), 159.0 (2 C), 161.6, 162.0, 168.7, 172.6; HRMS (ESI$^+$) m/z 1241.4970 ($C_{63}H_{72}N_{10}O_{15}SH$ [M + H]$^+$ requires 1241.4972).

(S)-2-((2S,4R)-4-Azido-1-(phenylsulfonyl)pyrrolidine-2-carbox-amido)-3-(4-((pyrrolidine-1-carbonyl)oxy)phenyl)propanoic acid (23). The methyl ester **18** (420 mg, 0.737 mmol) in EtOH (10 ml) was treated with 0.2 M NaOH (4.05 ml, 0.811 mmol) and stirred at rt for 1 h. The mixture was concentrated under reduced pressure to remove EtOH and the aqueous phase acidified with 10% HCl. The aqueous phase was extracted with CHCl$_3$ (4 × 10 ml) and the combined organic phases were washed with brine, dried (MgSO$_4$) and concentrated under reduced pressure. The crude material was purified by flash chromatography (10% MeOH–CH$_2$Cl$_2$ with 0.5% AcOH) to give acid **23** (384 mg, 94%) as a pale yellow foam, $[\alpha]_D$ −0.7 (c 1.00 in CHCl$_3$); δ_H (400 MHz, CDCl$_3$) 1.67–1.73 (1 H, m), 1.89–1.96 (5 H, m), 3.10 (1 H, dd, J = 8.0, 13.8 Hz), 3.21 (1 H, dd, J = 4.0, 11.5 Hz), 3.38 (1 H, dd, J = 5.3, 14.0 Hz), 3.44–3.55 (5 H, m), 3.81 (1 H, m), 4.11 (1 H, t, J = 6.5 Hz), 4.89 (1 H, m), 7.05, 7.22 (4 H, 2 × d, J = 8.0 Hz), 7.41 (1 H, d, J = 6.8 Hz), 7.53–7.64 (3 H, m), 7.85 (2 H, d, J = 7.5 Hz); δ_C (100 MHz, CDCl$_3$) 25.0, 25.8, 36.1, 36.8, 46.5, 46.6, 53.2, 53.9, 58.9, 61.2, 122.0 (2 C), 128.0 (2 C), 129.4 (2 C), 130.5 (2 C), 133.6, 133.7, 136.0, 150.5, 153.6, 170.9, 173.7; ν/cm^{-1} 3329, 2977, 2881, 2105, 1706, 1672; HRMS (ESI$^+$) m/z 557.1817 ($C_{25}H_{29}N_7O_6S$ [M + H]$^+$ requires 557.1813).

R-BC154 (25). The azide **23** (12 mg, 22 μmol) and N-propynyl sulforhodamine B **24** (14 mg, 24 μmol) in DMF (2 ml) were treated with CuSO$_4$ (86 μl, 0.86 μmol, 0.01 M in H$_2$O), sodium ascorbate (430 μl, 4.3 μmol, 0.01 M in H$_2$O) and tris[[(1-benzyl-1H-1,2,3-triazol-4-yl)methyl]amine (TBTA) (108 μl, 1.08 μmol, 0.01 M in DMF). The mixture was stirred at 60 °C for 2 h at which point TLC indicated formation of a new fluorescent product. The mixture was concentrated under reduced pressure and the residue partly purified by flash chromatography (40 : 10 : 1 CHCl$_3$–MeOH–H$_2$O with 0.5% AcOH). This material was further purified by HPLC (50%–98% MeCN–H$_2$O (0.1% TFA) gradient over 15 minutes; R_t = 14.9 min) to give pure **25** (10.6 mg, 43%) as a purple glass, δ_H (400 MHz, d_4-methanol) 1.27–1.31 (12 H, dt, J = 7.0, 3.5 Hz), 1.91–1.98 (4 H, m), 2.29–2.35 (1 H, m), 2.71–2.78 (1 H, m), 3.08 (1 H, dd, J = 7.5, 13.8 Hz), 3.22 (1 H, dd, J = 5.3, 13.8 Hz), 3.41 (2 H, t, J = 6.5 Hz), 3.54 (2 H, t, J = 6.5 Hz), 3.63–3.70 (8 H, m), 3.85 (1 H, dd, J = 3.5, 12.0 Hz), 3.97 (1 H, dd, J = 5.6, 11.6 Hz), 4.21 (2 H, d, J = 1.4 Hz), 4.41 (1 H, t, J = 7.3 Hz), 4.72 (1 H, dd, J = 5.4, 7.5 Hz), 5.08 (1 H, m), 6.91 (2 H, t, J = 2.2 Hz), 6.98–7.04 (4 H, m), 7.11 (2 H, t, J = 9.0 Hz), 7.30 (2 H, d, J = 8.6 Hz), 7.40 (1 H, d, J = 8.0 Hz), 7.44 (2 H, t, J = 7.5 Hz), 7.58–7.68 (4 H, m), 8.00 (1 H, dd, J = 1.9, 8.0 Hz), 8.37 (1 H, d, J = 1.8 Hz); δ_C (100 MHz, d_4-methanol) 12.9 (4 C), 25.9, 26.7, 37.1, 37.6, 39.0, 46.8 (4 C), 47.5, 47.6, 54.8, 55.7, 60.3, 62.1, 97.0 (2 C), 115.0 (2 C), 115.26, 115.29, 122.9 (2 C), 123.9, 127.5, 128.6 (2 C), 129.3, 130.5 (2 C),

131.6 (2 C), 132.3, 133.8, 133.9, 134.4, 135.26, 135.34, 138.3, 144.1, 144.8, 146.9, 151.7, 155.2, 157.16, 157.17, 157.2, 157.8, 159.4, 173.1, 173.8; ν/cm^{-1} 3088–3418, 2977, 2876, 1711, 1649, 1588; HRMS (ESI$^+$) m/z 1174.3447 ($C_{55}H_{61}N_9NaO_{13}S_3$ [M + Na]$^+$ requires 1174.3443). For in $vitro$ and in $vivo$ testing, the free acid of **25** (11.7 mg, 9.97 μmol) was dissolved in 0.01 M NaOH (997 μl, 9.97 μmol) and the dark purple solution filtered through a 0.45 μm syringe filter unit. The product was lyophilised to give the sodium salt of **25** (11.6 mg, 99%) as a fluffy purple powder.

Flow cytometry

Flow cytometric analysis was performed using an LSR II (BD Biosciences) equipped as previously described.[18] Both carboxytetramethylrhodamine (compound **22**) and Lissamine Rhodamine B (R-BC154) were excited at 561 nm (yellow-green laser) and detected at 585 ± 20 nm. Fluorescence activated cell sorting of haemopoietic progenitor cells was performed using a Cytopeia Influx (BD Biosciences) cell sorter equipped as previously described.[18]

Cell lines

Stable LN18 cells (ATCC number: CRL-2610) over-expressing integrin $\alpha_4\beta_1$ (LN18 $\alpha_4\beta_1$) or $\alpha_9\beta_1$ (LN18 $\alpha_9\beta_1$) were generated by retroviral transduction using the pMSCV-hITGA4-IRES-hITGB1 and pMSCV-hITGA9-IRES-hITGB1 vectors as previously described.[18] Transduced cells were selected by two rounds of FACS using 2.5 μg ml^{-1} PE-Cy5-conjugated mouse-anti-human α_4 antibody (BD Bioscience) or 20 μg ml^{-1} of mouse-anti-human $\alpha_9\beta_1$ antibody (Millipore) in PBS–2% FBS, followed by 0.5 μg ml^{-1} of PE-conjugated goat-anti-mouse IgG (BD Bioscience). Silencing of α_4 expression in LN18 and LN18 $\alpha_9\beta_1$ cells was performed as described above using pSM2c-shITGA4 (Open Biosystems). α_4-silenced LN18 cells (control cell line; LN18 SiA$_4$) and LN18 $\alpha_9\beta_1$ (LN18 $\alpha_9\beta_1$ SiA$_4$) were negatively selected for α_4 expression using FACS.

Immunohistochemistry

Antibody staining. LN18 SiA$_4$ (control cell line), LN18 $\alpha_4\beta_1$, and LN18 $\alpha_9\beta_1$ cells were stained with 2.5 μg ml^{-1} of mouse-anti-human α_4 antibody (BD Bioscience), 4 μg ml^{-1} of mouse-anti-human $\alpha_9\beta_1$ antibody (Millipore) or 4 μg ml^{-1} of mouse isotype control (BD Bioscience) in PBS–2% FBS for one hour, followed by 5 μg ml^{-1} of Alexa Fluor 594 conjugated goat-anti-mouse IgG1 for 1 h and then washed with PBS–2% FBS three times.

R-BC154 (25) staining. Cultured LN18 SiA$_4$ (control cell line), LN18 $\alpha_4\beta_1$, and LN18 $\alpha_9\beta_1$ cells were treated with R-BC154 (50 nM) in TBS–2% FBS (50 mM TrisHCl, 150 mM NaCl, 2 mM glucose, 10 mM Hepes, pH 7.4) containing 1 mM CaCl$_2$–MgCl$_2$ or 1 mM MnCl$_2$) and incubated for 20 min at 37 °C and then washed with TBS–2% FBS three times. The stained cells were fixed with 4% paraformaldehyde in PBS for 5 min, washed with water three times and then stained with 2.5 μg ml^{-1} of DAPI. The cells were mounted in Vectorshield, washed with water, coverslipped and stored at 4 °C overnight

976 | $Org. Biomol. Chem.$, 2014, **12**, 965–978

This journal is © The Royal Society of Chemistry 2014

before images were taken under fluorescent microscope (Olympus BX51).

Saturation binding experiments

Cultured $\alpha_4\beta_1$, $\alpha_9\beta_1$ and control LN18 cells (0.5×10^6 cells) were treated with 100 µl of either compound **22** or **25** (R-BC154) at 0, 1, 3, 10, 30 and 100 nM in TBS–2% FBS (containing either no cations, 1 mM CaCl$_2$–MgCl$_2$ or 1 mM MnCl$_2$). The cells were incubated at 37 °C for 60 min, washed once with TBS–2% FBS, dry pelleted and resuspended in the relevant binding buffer for flow cytometric analysis. Mean channel fluorescence was plotted against concentration and fitted to a one-site saturation ligand binding curve using GraphPad Prism 6. The dissociation constant, K_d was determined from the curves.

Off-rate kinetics measurements

Eppendorf vials containing $\alpha_4\beta_1$ or $\alpha_9\beta_1$ LN18 cells (0.5×10^6 cells) were treated with 50 nM of R-BC154 (100 µl in TBS–2% FBS containing either 1 mM CaCl$_2$–MgCl$_2$ or 1 mM MnCl$_2$ at 37 °C until for 30 min, washed once with the relevant binding buffer and dry pelleted. The cells were treated with 500 nM of an unlabelled competing inhibitor (100 µl, in TBS–2% FBS containing either 1 mM CaCl$_2$–MgCl$_2$ or 1 mM MnCl$_2$) at 37 °C for the times indicated (0, 2.5, 5, 15, 30, 45, 60 min). The cells were diluted with cold TBS–2% FBS (containing the relevant cations), pelleted by centrifugation, washed once and resuspended (~200 µl) in binding buffer for flow cytometric analysis. Mean channel fluorescence was plotted against time and the data was fitted to either a one-phase or two-phase exponential decay function using GraphPad Prism 6. The off-rate, k_{off} was extrapolated from the curves.

On-rate kinetics measurements

Eppendorf vials containing $\alpha_4\beta_1$ or $\alpha_9\beta_1$ LN18 cells (0.5×10^6 cells) in 50 µl TBS–2% FBS containing either 1 mM CaCl$_2$–MgCl$_2$ or 1 mM MnCl$_2$ were pre-activated in a heating block for 20 min at 37 °C. 100 nM R-BC154 (50 µl – final concentration = 50 nM) in the relevant TBS–2% FBS (with relevant cations) was added to each tube and after 0, 0.5, 1, 2, 3, 5, 10, 15 and 20 min incubation at 37 °C, the tubes were quenched by the addition of 3 ml of TBS–2% FBS (with relevant cations). The cells were washed once TBS–2% FBS (with relevant cations), pelleted by centrifugation and resuspended (200 µl) in the relevant binding buffer for flow cytometric analysis. Mean channel fluorescence was plotted against time and the data was fitted to either a one-phase or two phase association function using GraphPad Prism 6. The observed on-rate, k_{obs} was extrapolated from the curves and k_{on} was calculated using $(k_{obs} - k_{off})/[\text{R-BC154} = 50 \text{ nM}]$.

Mice

C57Bl/6 mice were bred at Monash Animal Services (Monash University, Clayton, Australia). Mice were 6–8 weeks old and sex-matched for experiments. All experiments were approved by Monash Animal Research Platform ethics committee (MARP/2012/128).

In vivo bone marrow binding assay

R-BC154 (**25**) in PBS (10 mg kg^{-1}) was injected intravenously into C57 mice. After 5 min, bone marrow cells were isolated as previously described.[41,42] Briefly, one femur, tibia and iliac crest were excised and cleaned of muscle. After removing the epi- and metaphyseal regions, bones were flushed with PBS–2% FBS to obtain whole bone marrow, which were washed with PBS–2% FBS and then immunolabelled for flow cytometry. For analysis of R-BC154 (**25**) binding, the following antibody combinations were chosen to minimise emission spectra overlap. For staining progenitor cells (LSK; Lineage$^-$Sca-1$^+$c-kit$^+$) and HSC (LSKSLAM; LSKCD150$^+$CD48$^-$), cells were labelled with a lineage cocktail (CD3, Ter-119, Gr-1, Mac-1, B220; all antibodies APC-Cy7 conjugated), anti-Sca-1-PB, anti-c-kit-AF647, anti-CD48-FITC and anti-CD150-BV650.

For assessing R-BC154 binding on sorted populations of progenitor cells (LSK cells), whole bone marrow was harvested from untreated and treated (R-BC154; 10 mg kg^{-1}) mice (3 mice per group). Lineage positive cells were immunolabelled using a lineage cocktail (B220, Gr-1, Mac-1 and Ter-119) and then removed by immunomagnetic selection with sheep anti-rat conjugated Dynabeads (Invitrogen) according to the manufacturer's instructions. The resultant lineage depleted cells were stained with anti-Sca-1-PB and anti-c-kit-FITC. Immunolabelled cells were sorted on Sca-1$^+$c-kit$^+$ using a Cytopeia Influx (BD Biosciences) cell sorter and imaged using an Olympus BX51 microscope.

References

1 R. O. Hynes, *Cell*, 1992, **69**, 11–25.
2 E. A. Clark and J. S. Brugge, *Science*, 1995, **268**, 233–239.
3 D. Cox, M. Brennan and N. Moran, *Nat. Rev. Drug. Discovery*, 2010, **9**, 804–820.
4 J. D. Humphries, A. Byron and M. J. Humphries, *J. Cell Sci.*, 2006, **119**, 3901–3903.
5 K. J. Bayless, G. A. Meininger, J. M. Scholtz and G. E. Davis, *J. Cell Sci.*, 1998, **111**, 1165–1174.
6 R. R. Lobb and M. E. Hemler, *J. Clin. Invest.*, 1994, **94**, 1722–1728.
7 R. R. Lobb and S. P. Adams, *Expert Opin. Invest. Drugs*, 1999, **8**, 935–945.
8 M. Millard, S. Odde and N. Neamati, *Theranostics*, 2011, **1**, 154–188.
9 Y. Taooka, J. Chen, T. Yednock and D. Sheppard, *J. Cell Biol.*, 1999, **145**, 413–420.

This journal is © The Royal Society of Chemistry 2014

Org. Biomol. Chem., 2014, **12**, 965–978 | 977

10 Y. Yokosaki, N. Matsuura, T. Sasaki, I. Murakami, H. Schneider, S. Higashiyama, Y. Saitoh, M. Yamakido, Y. Taooka and D. Sheppard, *J. Biol. Chem.*, 1999, **274**, 36328–36334.

11 H. Takahashi, T. Isobe, S. Horibe, J. Takagi, Y. Yokosaki, D. Sheppard and Y. Saito, *J. Biol. Chem.*, 2000, **275**, 23589–23595.

12 R. B. Pepinsky, R. A. Mumford, L. L. Chen, D. Leone, S. E. Amo, G. Van Riper, A. Whitty, B. Dolinski, R. R. Lobb, D. C. Dean, L. L. Chang, C. E. Raab, Q. Si, W. K. Hagmann and R. B. Lingham, *Biochemistry*, 2002, **41**, 7125–7141.

13 N. E. Vlahakis, B. A. Young, A. Atakilit, A. E. Hawkridge, R. B. Issaka, N. Boudreau and D. Sheppard, *J. Biol. Chem.*, 2007, **282**, 15187–15196.

14 E. M. Walsh, R. Kim, L. Del Valle, M. Weaver, J. Sheffield, P. Lazarovici and C. Marcinkiewicz, *Neuro-Oncology*, 2012, **14**, 890–901.

15 P. Singh, C. Chen, S. Pal-Ghosh, M. A. Stepp, D. Sheppard and L. Van De Water, *J. Invest. Dermatol.*, 2009, **129**, 217–228.

16 I. Staniszewska, S. Zaveri, L. Del Valle, I. Oliva, V. L. Rothman, S. E. Croul, D. D. Roberts, D. F. Mosher, G. P. Tuszynski and C. Marcinkiewicz, *Circ. Res.*, 2007, **100**, 1308–1316.

17 J. Teixido, M. E. Hemler, J. S. Greenberger and P. Anklesaria, *J. Clin. Invest.*, 1992, **90**, 358–367.

18 J. Grassinger, D. N. Haylock, M. J. Storan, G. O. Haines, B. Williams, G. A. Whitty, A. R. Vinson, C. L. Be, S. H. Li, E. S. Sorensen, P. P. L. Tam, D. T. Denhardt, D. Sheppard, P. F. Choong and S. K. Nilsson, *Blood*, 2009, **114**, 49–59.

19 T. D. Schreiber, C. Steinl, M. Essl, H. Abele, K. Geiger, C. A. Muller, W. K. Aicher and G. Klein, *Haematol.-Hematol. J.*, 2009, **94**, 1493–1501.

20 P. Ramirez, M. P. Rettig, G. L. Uy, E. Deych, M. S. Holt, J. K. Ritchey and J. F. DiPersio, *Blood*, 2009, **114**, 1340–1343.

21 S. Choi, G. Vilaire, C. Marcinkiewicz, J. D. Winkler, J. S. Bennett and W. F. DeGrado, *J. Med. Chem.*, 2007, **50**, 5457–5462.

22 M. W. Miller, S. Basra, D. W. Kulp, P. C. Billings, S. Choi, M. P. Beavers, O. J. T. McCartye, Z. Y. Zou, M. L. Kahn, J. S. Bennett and W. F. DeGrado, *Proc. Natl. Acad. Sci. U. S. A.*, 2009, **106**, 719–724.

23 O. E. Hutt, S. Saubern and D. A. Winkler, *Bioorg. Med. Chem.*, 2011, **19**, 5903–5911.

24 S. Venkatraman, J. Lim, M. Cramer, M. F. Gardner, J. James, K. Alves, R. B. Lingham, R. A. Mumford and B. Munoz, *Bioorg. Med. Chem. Lett.*, 2005, **15**, 4053–4056.

25 R. B. Pepinsky, W. C. Lee, M. Cornebise, A. Gill, K. Wortham, L. L. Chen, D. R. Leone, K. Giza, B. M. Dolinski, S. Perper, C. Nickerson-Nutter, D. Lepage, A. Chakraborty, E. T. Whalley, R. C. Petter, S. P. Adams, R. R. Lobb and D. M. Scott, *J. Pharmacol. Exp. Ther.*, 2005, **312**, 742–750.

26 L. S. Lin, T. Lanza, J. P. Jewell, P. Liu, C. Jones, G. R. Kieczykowski, K. Treonze, Q. Si, S. Manior, G. Koo, X. C. Tong, J. Y. Wang, A. Schuelke, J. Pivnichny, R. Wang, C. Raab, S. Vincent, P. Davies, M. MacCoss, R. A. Mumford and W. K. Hagmann, *J. Med. Chem.*, 2009, **52**, 3449–3452.

27 J. A. Smith, G. P. Savage and O. E. Hutt, *Aust. J. Chem.*, 2011, **64**, 1509–1514.

28 C. E. Jakobsche, P. J. McEnaney, A. X. Zhang and D. A. Spiegel, *ACS Chem. Biol.*, 2012, **7**, 315–320.

29 T. S. Reger, J. Zunic, N. Stock, B. W. Wang, N. D. Smith, B. Munoz, M. D. Green, M. F. Gardner, J. P. James, W. C. Chen, K. Alves, Q. Si, K. M. Treonze, R. B. Lingham and R. A. Mumford, *Bioorg. Med. Chem. Lett.*, 2010, **20**, 1173–1176.

30 C. W. Tornoe, C. Christensen and M. Meldal, *J. Org. Chem.*, 2002, **67**, 3057–3064.

31 V. V. Rostovtsev, L. G. Green, V. V. Fokin and K. B. Sharpless, *Angew. Chem., Int. Ed.*, 2002, **41**, 2596–2599.

32 T. C. Liu, J. R. Nedrow-Byers, M. R. Hopkins and C. E. Berkman, *Bioorg. Med. Chem. Lett.*, 2011, **21**, 7013–7016.

33 K. E. Beatty and D. A. Tirrel, *Bioorg. Med. Chem. Lett.*, 2008, **18**, 5995–5999.

34 A. H. Broderick, S. M. Azarin, M. E. Buck, S. P. Palecek and D. M. Lynn, *Biomacromolecules*, 2011, **12**, 1998–2007.

35 G. Delaittre, A. M. Greiner, T. Pauloehrl, M. Bastmeyer and C. Barner-Kowollik, *Soft Matter*, 2012, **8**, 7323–7347.

36 A. P. Mould, *J. Cell Sci.*, 1996, **109**, 2613–2618.

37 E. F. Plow, T. K. Haas, L. Zhang, J. Loftus and J. W. Smith, *J. Biol. Chem.*, 2000, **275**, 21785–21788.

38 J. Grassinger, D. N. Haylock, B. Williams, G. H. Olsen and S. K. Nilsson, *Blood*, 2010, **116**, 3185–3196.

39 A. B. Pangborn, M. A. Giardello, R. H. Grubbs, R. K. Rosen and F. J. Timmers, *Organometallics*, 1996, **15**, 1518–1520.

40 R. H. Andreatta, V. Nair and A. V. Roberston, *Aust. J. Chem.*, 1967, **20**, 2701–2713.

41 D. N. Haylock, B. Williams, H. M. Johnston, M. C. P. Liu, K. E. Rutherford, G. A. Whitty, P. J. Simmons, I. Bertoncello and S. K. Nilsson, *Stem Cells*, 2007, **25**, 1062–1069.

42 J. Grassinger, B. Williams, G. H. Olsen, D. N. Haylock and S. K. Nilsson, *Cytokine*, 2012, **58**, 218–225.

978 | *Org. Biomol. Chem.*, 2014, **12**, 965–978

This journal is © The Royal Society of Chemistry 2014